INVESTIGATING THE MAMMALIAN HEAT-SHOCK INDUCED UBIQUITINATION RESPONSE

by

AMALIA ROSE

B.Sc., The University of British Columbia (2015)

A THESIS SUBMITTED IN PARTIAL FULFILLMENT OF THE REQUIREMENTS FOR THE DEGREE OF

MASTER OF SCIENCE

in

THE FACULTY OF GRADUATE AND POSTDOCTORAL STUDIES

(Biochemistry and Molecular Biology)

THE UNIVERSITY OF BRITISH COLUMBIA

(Vancouver)

March 2018

Abstract

Aggregation of misfolded proteins in the cell is often indicative of a failing protein quality control system, whose responsibility is to mediate either the refolding or degradation of these aberrant proteins. Heat-shock (HS), which causes proteins to misfold, leads to a marked increase of the ubiquitination of proteins that display poor solubility in the cell. The E3 ubiquitin ligase Rsp5 has previously been shown to be the major ubiquitin ligase that targets cytosolic misfolded proteins upon HS in *S. cerevisiae*. Its closest mammalian orthologue, Nedd4-1, was also found to be responsible for increased ubiquitination upon HS in HeLa and MEF cells, however further work is needed to better characterize this response. Such characterization included looking at which proteins get ubiquitinated upon HS to then determine whether they share common characteristics such as cellular localization, and if they are newly synthesized versus pre-existing. Using diGly enrichment coupled with mass spectrometry, we identified over 300 proteins that were further ubiquitinated upon HS. An important portion of these proteins are localized in the nucleus, whereas proteins associated to the mitochondria are markedly under-represented. As well, proteins involved in processes such as pre-mRNA processing, cell cycle and SUMOylation were found to be enriched. Using a pulse-SILAC approach, we found that a large portion of proteins ubiquitinated after HS were pre-existing, whereas some were newly synthesized including ribosomal proteins. We also investigated the potential role of other Nedd4 family members in the HS ubiquitination response in Hek293 cells. Using shRNA, we found that the knockdown of the Itch E3, but not of Nedd4-1, caused a decrease of the HS-induced ubiquitination response in these cells. Accordingly, we also showed a reduced cell viability upon Itch knocked down under HS.

Lay Summary

Properly functioning proteins are vital to our health. If left unchecked, damaged proteins will start to aggregate, which not only stop them from carrying out their normal function, but may also impair other proteins within a cell. Protein aggregation is associated to several neurodegenerative diseases such as Parkinson's, and can also occur when a cell is under stress, such as heat-shock (HS). Our cells have developed several ways of destroying these damaged proteins, such as the ubiquitin-proteasome system (UPS). In the UPS, the faulty protein is tagged with ubiquitin, and can then be targeted to the proteasome for degradation. HS causes an increase of ubiquitin tagging and my primary objective is to further characterize this stress response. My work includes identifying what proteins are tagged with ubiquitin upon HS, and which enzyme causes these events. This will lead to insights on diseases caused by protein aggregation and potential therapeutic targets.

Preface

This dissertation is original and based on unpublished and independent work performed by the author, A. Rose. A segment of the introduction is also used for a review authored by A. Rose and to be published in a chapter book. The protein localization and abundance analysis in Chapter 3.1 was performed by E. Kuechler and he wrote the methods associated with this. The pulse SILAC diGly enrichment performed in Chapter 3.1 was aided by S. Kammoonah. N. Stoynov ran mass spectrometry (MS) samples on the Q-TOF and helped write the method associated with that. S. Colborne ran MS samples on the Orbitrap and C. Hughes helped write the method associated with that.

Table of Contents

List of Tables

List of Figures

List of Abbreviations

AIP4	Atrophin interacting protein 4
ATP	Adenosine triphosphate
CCT	Chaperonin containing TCP-1
CID	Collision-induced dissociation
DMEM	Dulbecco's modified Eagle medium
DMSO	Dimethyl sulfoxide
DUB	Deubiquitinase
E1	Ubiquitin activating enzyme
E2	Ubiquitin conjugating enzyme
E3	Ubiquitin ligase
EDTA	Ethylenediaminetetraacetic acid
ER	Endoplasmic reticulum
FBS	Fetal bovine serum
FITC	Fluorescein isothiocyanate
GLYGLY/DIGLY	Ubiquitin two C-terminal glycines
GO	Gene ontology
HECT	Homologous to the E6-AP carboxyl terminus
HEK	Human embryonic kidney
HEPES	4-(2-Hydroxyethyl) piperazine-1-ethanesulfonic acid
HERC	HECT and regulator of chromosome condensation 1 (RCC1)- containing
HS	Heat-shock
HSF1	Heat shock factor 1

HSP	Heat-shock protein
K	Lysine
KD	Knockdown
LB	Lysogeny broth
LC-MS/MS	Liquid chromatography coupled with tandem mass spectrometry
LIG3	DNA ligase 3
LRAD3	Low density lipoprotein receptor class A domain containing 3
MEF	Mouse embryonic fibroblast
mRNA	Messenger RNA
NEDD4	Neural precursor cell-expressed developmentally down-regulated protein 4
NEDD4L	NEDD4-like
NEDL1	Nedd4-like ubiquitin protein ligase-1
NEDL2	Nedd4-like ubiquitin protein ligase-2
NOP56P	Nucleolar protein 5A
NP-40	Nonyl phenoxypolyethoxylethanol
PARP1	Poly [ADP-ribose] polymerase 1
PBS	Phosphate-buffered saline
PMSF	Phenylmethylsulfonyl fluoride
PQC	Protein quality control
PTEN	Phosphatase and tensin homolog
PTM	Post-translational modification
Q-TOF	Quadrupole time of flight
RBR	RING-between-RING

RING	Really interesting new gene
RIPA	Radioimmunoprecipitation assay
RPM	Revolutions per minute
rRNA	Ribosomal RNA
SDS	Sodium dodecyl sulfate
shRNA	Short hairpin RNA
SILAC	Stable isotope labeling with amino acids in cell culture
SMURF1	SMAD ubiquitination regulatory factor 1
SMURF2	SMAD ubiquitination regulatory factor 2
S-phase	Synthesis phase
SUMO	Small ubiquitin-like modifier
TCEP	Tris(2-carboxyethyl) phosphine
TCL	Total cell lysate
TRC	The RNAi Consortium
Tris	Tris(hydroxymethyl)aminomethane
Ub	Ubiquitin
UPS	Ubiquitin proteasome system
UTR	Untranslated region
WT	Wild-type
WWP1	WW domain-containing protein 1
WWP2	WW domain-containing protein 2
XIC	eXtracted ion current
XRCC5	X-ray repair cross-complementing protein 5

Acknowledgements

First and foremost, I would like to thank Dr. Thibault Mayor for taking me onboard and guiding me throughout this project. Your dedication to your research and to the lab, and how you stay on top of everybody's project as well as have time for your family is truly inspiring. I would also like to thank Dr. Ivan Robert Nabi and Dr. Michel Roberge for being on my committee and providing me with valuable scientific insight.

Many thanks to Dr. Nikolay Stoynov for his MS expertise and willingness to always provide explanations. I would also like to thank Dr. Anna Prudova who I relied upon for cell culture help and advice, and to Dr. Avinash Persaud from SickKids for his cell culture help. Thank you to Shane Colborne for his assistance in running my MS samples. I want to acknowledge the generosity of Dr. Daniela Rotin from SickKids for gifting us with some of the cell lines and plasmids used in this project.

I would like to thank Dr. Erich Kuechler for doing all the bioinformatic analysis on my MS data, as well as Shaima Kammoonah for helping me with MS sample processing. Finally, I would like to thank the rest of the past and present Mayor lab members for helping me with different techniques/instruments, especially Dr. Sophie Comyn and Mang Zhu who were with me throughout the length of my project and helped make my time in the lab memorable.

Chapter 1 - Introduction

Cells are constantly expending a large amount of energy to maintain a functional proteome, as the accumulation of misfolded proteins can be disastrous[1]. Over 50 human pathologies (mainly neurodegenerative) are associated with protein aggregation, however recently, the accumulation of mutant proteins that misfold has also been thought to contribute to cancer, inflammation, and immune disorders[2]. Typically, the aggregation prone sequence within a protein is buried in the hydrophobic core. Upon misfolding, this region becomes exposed and the protein is then more likely to aggregate[3]. Many sporadic neurodegenerative diseases that have a higher incidence upon aging are the result of a cell's inability to dispose these misfolded protein aggregates in dying neurons. For instance, the aggregation of α-synuclein predominantly at the presynapse of dopaminergic neurons leads to synaptic dysfunction and neurodegeneration in Parkinson's disease and dementia with Lewy bodies[4]. A comprehensive understanding of how cells prevent these aggregates from forming and related diseases is crucial to develop future therapeutic approaches.

1.1. Heat-Shock Response

Cellular stresses such as heat-shock (HS) often result in the misfolding of proteins and the faulty assembly of protein complexes. HS involves subjecting the cell or organism to abnormally elevated temperatures, which then induces the HS response. It has been found however, that the HS response is a more general cell stress response, as it can be triggered by stresses other than heat[5]. Other conditions that trigger the HS response in a cell can come from a wide variety of sources, such as exposure to toxic chemicals, temperatures below a certain range, fever, infection, or the increase of cytotoxic proteins in cancer and neurodegenerative

diseases. The HS response consists of the rapid induction of hundreds of genes critical for cell survival, along with the repression of several thousands of other genes[6]. Many of these induced genes are molecular chaperones known as heat shock proteins (HSPs) which are critical for survival. This induction is orchestrated by heat shock factors (HSFs) and more specifically HSF1, that binds to HSP promoters and recruits co-factors that increase the transcription of HSPs[6]. HSF1 exists as an inactive monomer under normal conditions but trimerizes and becomes active upon the induction of HS[6].

HS can cause many detrimental effects to the cell that include cytoskeleton defects, which in turn lead to the incorrect localization of organelles and disrupt signalling pathways, an increase in membrane fluidity, and a global decrease in translation[5]. This decrease in translation is due in part to the inhibition of the formation of the eIF4F complex, an essential component of eukaryotic translation, as well as widespread inhibition of posttranscriptional splicing[7,8]. The combination of all these effects often leads to an arrest in the cell cycle in dividing cells. The severity of the stress also depends on the cell cycle stage. For example, cells undergoing mitosis or in S-phase (synthesis phase) are more sensitive to HS[9]. Depending on the temperature and length of HS, these factors can lead to loss of viability and cell death through apoptosis.

1.1 Protein Quality Control

Several mechanisms and pathways, collectively known as protein quality control (PQC), oversee the proper folding and, if necessary, degradation of faulty proteins to maintain protein homeostasis. The role of PQC mechanisms is particularly critical during a stress like HS (Figure 1.1). One of the immediate responses to protein misfolding is to decrease protein synthesis and consequently increase the availability of chaperones that normally assist the

folding of nascent polypeptides[1]. Chaperones bind to non-native proteins to prevent them from irreversible aggregation and keep them within a productive folding path. In some other cases, chaperones can also assist protein degradation, such as in chaperone mediated autophagy[10]. In addition to decreased protein translation, the HS response induces the expression of heat shock proteins (HSPs) that act as molecular chaperones to stabilize protein conformation and assist with the proper folding, assembly, and disassembly of protein complexes. That increased folding capacity allow for a temporary thermotolerance to block apoptotis[9].

Consequently, proteins that are unable to be folded into a functional state are targeted for degradation through autophagy or the ubiquitin proteasome system (UPS). In autophagy, a large variety of cell components, ranging from proteins to entire organelles undergo degradation in the lysosome. In contrast, proteins are degraded by the proteasome once tagged with polyubiquitin within the UPS[11]. The two pathways have also been shown to have overlapping substrates and to be able to compensate for each other when one of them is compromised[12]. In fact, proteins tagged with ubiquitin can also be targeted to the autophagy machinery instead of the proteasome[13]. The type of ubiquitin chains, localization and cargo ubiquitin binding proteins determine which proteolytic path is undertaken by a given conjugated protein. It has previously been suggested that upon HS, mostly newly-synthesized proteins are targeted for proteasomal degradation due to their instability and propensity to misfold, and pre-existing proteins mainly get targeted for lysosomal degradation regardless of HS[14]. For the remainder of this thesis however, the focus will be mainly on the UPS.

1.2. Ubiquitin Proteasome System

The UPS is a major component of PQC and involves the tagging of a protein with ubiquitin, otherwise known as ubiquitination, which signals it to a specific process or

component of the cell such as the proteasome where it gets degraded[15]. Ubiquitin is a highly conserved 76 amino acid long protein that can be conjugated via its C-terminus to other polypeptides, mostly on lysine residues or its N-terminus[16]. Ubiquitin contains seven lysine residues (K6, K11, K27, K29, K33, K48, and K63) and an amino group at its N-terminus (M1) which can be conjugated by other ubiquitin molecules to form a poly-ubiquitin chain[15]. These chains can either be connected through the same lysine, have mix linkage types, or even be branched where a single ubiquitin within the chain is modified with two ubiquitin molecules[17]. Although many lysine linkages target the conjugated protein for degradation, some mediate proteasomal degradation in a more prevalent manner[15]. For example, K48 linked chains typically signal proteins for degradation by the 26S proteasome whereas K63 linkages have a role in autophagy[18].

Ubiquitin (Ub) is added to target substrates sequentially through a multi-enzyme cascade. Initially, E1 enzymes activate the C-terminus of ubiquitin with the use of adenosine triphosphate (ATP) by forming a high energy E1~Ub thioester adduct. In humans, two E1 enzymes, are responsible for all ubiquitin activation. Once activated, ubiquitin is transferred from the E1 to E2 enzymes, otherwise known as ubiquitin conjugating enzymes. The E2s transfer ubiquitin from E1 enzymes to the catalytic cysteine of E3 ubiquitin ligases or directly to substrates associated to E3s (Figure 1.2)[19]. E3 ligases are responsible for substrate specificity and they typically catalyze the transfer of ubiquitin molecules from E2 enzymes to lysine residues on the substrate. There are 3 types of E3 ligases: those that contain a Really Interesting New Gene (RING) finger catalytic domain, a RING-Between-RING (RBR) domain, and ligases that contain a Homologous to the E6-AP Carboxyl Terminus (HECT) domain[20]. RING E3s are scaffolds that bring the E2 near the substrates to facilitate the transfer

of ubiquitin to the substrate[21]. By contrast, HECT domains contain a catalytic cysteine that forms an intermediate thioester bond with the ubiquitin C-terminus before catalysing substrate ubiquitination[21]. RBR E3s contain two RING domains as well as a catalytic cysteine in one of the RINGs that functions similarly to HECT E3s [20]. The HECT E3 ligases can be divided into 3 groups: the neural precursor cell-expressed developmentally down-regulated protein 4 (Nedd4) family (the focus of this thesis), the HECT and regulator of chromosome condensation 1 (RCC1)- containing (HERC) family, and other HECTs[21]. Ubiquitin conjugation is a reversible process where deubiquitinases (DUBs) act to remove ubiquitin from modified proteins, causing ubiquitination to be a highly dynamic process[22]. In humans, there are more than 30 E2s, over 600 E3s, and approximately 90 DUBs, creating a complex system[23].

As previously mentioned, proteins conjugated with a particular type of polyubiquitin chain are targeted to the proteasome complex, where they are subsequently degraded. It was first thought that a K48 polyubiquitin chain must be a minimum of four molecules in length for efficient binding to the proteasome[24], however recently it has been reported that multi mono-ubiquitinated substrates can also be targeted to the proteasome, as well as substrates conjugated to K11-chains[13]. The 26S proteasome, consists of a 20S catalytic core particle capped on either side by a 19S regulatory particle[25]. The latter particle recognizes ubiquitinated client proteins, removes the ubiquitin chains, unfolds client proteins, and translocate them into the 20S. The 19S lid contains DUBs which remove the ubiquitin resulting in the recycling of ubiquitin in the cell[26]. The 20S has a barrel structure containing proteases that cleave the peptide bonds of the incoming proteins, generating oligopeptides long of 3 to 15 amino acids, and thus degrading their substrates[25].

1.3. Nedd4 Family Heat-Shock Ubiquitination Response

As HS causes proteins to misfold, it also induces an increase in polyubiquitination which is illustrated by a drop in the levels of free ubiquitin and the corresponding formation of high molecular weight conjugate species[27]. It was also shown that HS causes an increased degradation of misfolded proteins by the proteasome[14]. In a previous study, we discovered a novel and conserved protein quality control degradation pathway in which Rsp5 and Nedd4-1 are the main ubiquitin ligases that target proteins for proteasomal degradation[28]. The evidence for Rsp5 came from a lack of HS-dependent increased ubiquitination when using an Rsp5 temperature sensitive mutant, as well as a rescue of these levels when reintroducing Rsp5 into cells in which Rsp5 expression had been reduced. It was also found that Rsp5 substrates upon HS contain PY motifs and that association of the Hsp40 chaperone Ydj1 with Rsp5 mediates their ubiquitination. These results indicate that Rsp5 recognizes misfolded proteins through a bipartite model: substrates containing PY motifs are directly recognized by Rsp5 and/or recruited by Ydj1. In a separate Rsp5 study, we screened for other factors involved in the heat-shocked induced ubiquitination response, and found that the Ubp2/Ubp3 deubiquitinating enzymes are required for the proteasome degradation of cytosolic misfolded proteins in yeast[29]. Rsp5 mostly synthesizes K63-linked ubiquitin chains, however the targeted substrates for degradation upon heat-shock are conjugated to K48-linked chains. Our results indicate that Rsp5 changes its specificity upon HS to synthesise more K48-linked chains and Ubp2/Ubp3 promotes the assembly of K48-chains by having an increased association with Rsp5 under heat stress and thus removing K63 chains, preventing their formation.

Both Rsp5 (*Saccharomyces cerevisiae)* and its closest mammalian orthologue Nedd4-1 belong to the Nedd4 family of E3 ligases that can be found throughout eukaryotes. Nedd4

E3 ligases all share common domains and organizational features. They are comprised of an N-terminal C2 domain, a catalytic C-terminal HECT domain, and two to four WW domains[30]. The N-terminal C2 domain interacts with phospholipids and regulates cellular localization, by mediating binding to cell membranes[21]. The WW domains are involved in substrate recognition by recognizing and binding to so called PY motifs that are short linear motifs, such as PPxY and LPxY (in which x can be any amino acid). The PY motifs are either present on the targets or substrate adaptor proteins. As stated previously, the HECT domain mediates the transfer of the ubiquitin onto the substrate through a catalytic cysteine. This domain is bilobal, where the lobe closest to the N-terminus (N-lobe) binds the E2, upon which the ubiquitin molecule is transferred to the catalytic cysteine on the C-lobe (lobe proximal to the C-terminus)[21]. The ubiquitin is then transferred to lysine residues of the HECT ligase substrates that are recruited by one or more WW domain(s). To allow regulation of these E3s, they mainly reside in an inactive form in the cell, where access to the ubiquitin binding site is blocked, and require external proteins to relieve them of their auto-inhibitory state. There have been different proposed inhibitory mechanisms, such as the C2 domain binding to the HECT domain[31], a WW domain binding to the HECT domain[32,33], and the linker between WW domains locking the HECT domain in an inactive state[34]. Depending on the HECT E3, they have also been shown to be activated by the binding of other proteins[31–33] or by being phosphorylated[33,34].

Our previous studies show that Nedd4-1 is the main E3 ligase responsible for increased ubiquitination in mammalian cells upon HS, however there was not a complete abrogation of this increase in polyubiquitination in the absence of Nedd4-1, especially in HeLa cells[28]. There are nine members of the Nedd4 E3 ligase family in humans including Nedd4-1, Nedd4-Like

(Nedd4L), SMAD Ubiquitination Regulatory Factor 1 (Smurf1), SMAD Ubiquitination Regulatory Factor 2 (Smurf2), Itch, WW Domain-Containing Protein 1 (WWP1), WW Domain-Containing Protein 2 (WWP2), Nedd4-like Ubiquitin Protein Ligase-1 (NedL1), and Nedd4-like Ubiquitin Protein Ligase-2 (NedL2) (Figure 1.3)[35]. Nedd4-1 is widely expressed in mammalian tissues, where it plays key roles in cell proliferation through insulin signalling, the regulation of the tumor suppressor Phosphatase and Tensin Homolog (PTEN), regulation of α-synuclein, T-cell function, and may even play a significant role in cancer[31]. Based on their HECT domains, Nedd4-1 and Nedd4L are closely related and even have been shown to share substrates, indicating that they partially share a redundant role[36]. Itch, although not as closely related to Nedd4-1 as Nedd4L, can be activated by Low Density Lipoprotein Receptor Class A Domain Containing 3 (LRAD3) which also modulates Nedd4-1 activity[37]. Itch is also expressed in T-cells and shares common substrates with Nedd4-1[31]. Although each of the Nedd4 family members have been shown to have distinct roles in the cell, due to their common domains it is possible that some of them may have either overlapping roles in the HS ubiquitination response or they could target different set of proteins during the HS response.

1.4. Heat-Shock Ubiquitinome

Whereas the increased ubiquitination following HS has been well characterized in yeast cells, it remains unclear which proteins are targeted in mammalian cells. There have been studies investigating the behaviour of individual proteins, such as with the turnover of the cystic fibrosis transmembrane conductance regulator under HS conditions[38]. System-wide analysis of post-translational modifications (PTMs) however can illuminate previously unknown substrates and give a broader picture of the processes that this PTM is involved in during HS. Such analysis has been done with SUMOylation, where hundreds of previously

unknown substrates of Small Ubiquitin-like Modifier (SUMO) proteins were discovered following HS[39,40]. These studies indicate that SUMO-2 is an important early signaling molecule in the cellular defense against HS. Doing a similar study with ubiquitination could not only uncover substrates of the Nedd4 family, but give insight into key processes involved in the mammalian HS ubiquitination response.

Over the last 15 years, significant strides have been made towards obtaining a system-wide view of the 'ubiquitinome'—the ensemble of ubiquitinated proteins in a given cell or tissue. Most methods have relied on proteomic approaches. As for most protein mass spectrometry methods, a bottom-up approach is typically used to analyze ubiquitinated proteins, where proteins are indirectly analyzed through their corresponding peptides that are generated by proteolysis[41]. Upon trypsin digestion of a ubiquitin-conjugated protein, a signature peptide is produced consisting of the last two C-terminal glycines of ubiquitin (GlyGly, also called a diGly or the ubiquitin remnant) that remain covalently attached to the lysine residue of the target protein. As trypsin is unable to cleave after the conjugated lysine, the signature peptide contains both a missed cleavage and a 114.04 kDa mass shift at the modified lysine, which can then be readily identified during the database search[42].

Although trypsinized ubiquitinated proteins produce unique peptides, a major challenge of identifying these conjugation sites is due to the substoichiometric nature of these modifications[43]. Indeed, a large proportion of the modified proteins are targeted for proteolysis and, when not degraded, DUBs can reverse the modification. Therefore, the transient nature of ubiquitination makes it particularly difficult for identification by mass spectrometry. The enrichment of ubiquitinated proteins or peptides prior to mass spectrometry analysis is therefore critical for a successful large-scale analysis of the ubiquitin proteome.

In past years, major breakthroughs have been achieved in the identification of ubiquitination sites by enriching for conjugates at the peptide level as opposed to at the protein level. The purification of conjugated peptides has been enabled by the introduction of antibodies that recognize the signature GlyGly motif that remains bonded to lysine of ubiquitinated proteins after trypsinization (Figure 1.4). Xu *et al.* generated an anti-diglycyl-lysine (K-ε-GG) antibody to immunoprecipitate the GlyGly-modified lysine at a high yield, leading to the discovery of more than 150 previously unknown ubiquitinated proteins[44]. Importantly, this purification method hinges on endogenous ubiquitin and thus avoids potential off-target effects from the ectopic expression of tagged ubiquitin.

The introduction of the antibody-based enrichment approach led to the identification of thousands of new ubiquitination sites in mammalian tissue culture cells and tissues. Dr. Steve Gygi and colleagues used this antibody with an improved enrichment method to identify ~19,000 ubiquitin sites in ~5,000 proteins in HCT116 cells, which was a marked improvement on the ~1,000 previously identified sites[45]. They then also quantified temporal changes in the ubiquitin proteome in response to proteasome inhibition. By applying this proteotoxic stress, they identified a large class of proteins that accumulate as a result, as well as proteins that remain unchanged or whose diGly abundance decreases. They utilized this inhibition to identify cullin-RING ligase (CRL) substrates, and found that many proteasome targets were newly synthesized proteins. Importantly, they performed a series of experiments to show that the vast majority of the identified sites (>95%) were derived from ubiquitin and not Nedd8 conjugation. Using an independently generated anti-K-ε-GG antibody, the Choudhary lab was able to identify ~20,000 ubiquitination sites in mice, as well as ~11,000 sites in HEK293 cells[46,47]. By comparing these high numbers of sites, the authors of these studies showed that

these antibodies do not have any strong bias towards any particular sequence that surrounds the diGly motif, illustrating the efficacy of this approach[45,46]. Because HS induces a large increase of ubiquitination in tissue culture cells, we reasoned that the GlyGly enrichment method may be well suited to study changes in the ubiquitinome under HS conditions.

1.5. Thesis Investigation

The role of Rsp5 in the HS ubiquitination response has been well characterized in *Saccharomyces cerevisiae* yeast cells by our lab, however less effort has been deployed by us and others to characterize the mammalian ubiquitination HS response. Thus, the goal of my thesis work was to better characterize the HS response in mammalian tissue culture cell in order to determine how well conserved this pathway is. In Chapter 3.1, we first determined which proteins are ubiquitinated upon HS in mammalian tissue culture cells using proteomic approaches. We hypothesized that these targeted proteins share common characteristics that may lead to their ubiquitination and therefore applied a computational approach to assess their cell localization and abundance. Surprisingly we found that down regulation of Nedd4-1 in Hek293 cells did not affect the HS response. Based on our previous work in yeast, we hypothesized that other members of the Nedd4 family member could participate in the stress response. Using a short hairpin RNA (shRNA) knockdown (KD) approach, we evaluated the role of all 9 family members in the HS ubiquitination response, which is described in Chapter 3.2. Finally, in Chapter 3.3, we confirmed that Need4-1 is implicated in the HS ubiquitination response and further characterized its role in HS conditions. All together, we were able to identify a group of proteins that are ubiquitinated upon HS in Hek293 cells and show that Itch plays a role in their ubiquitination.

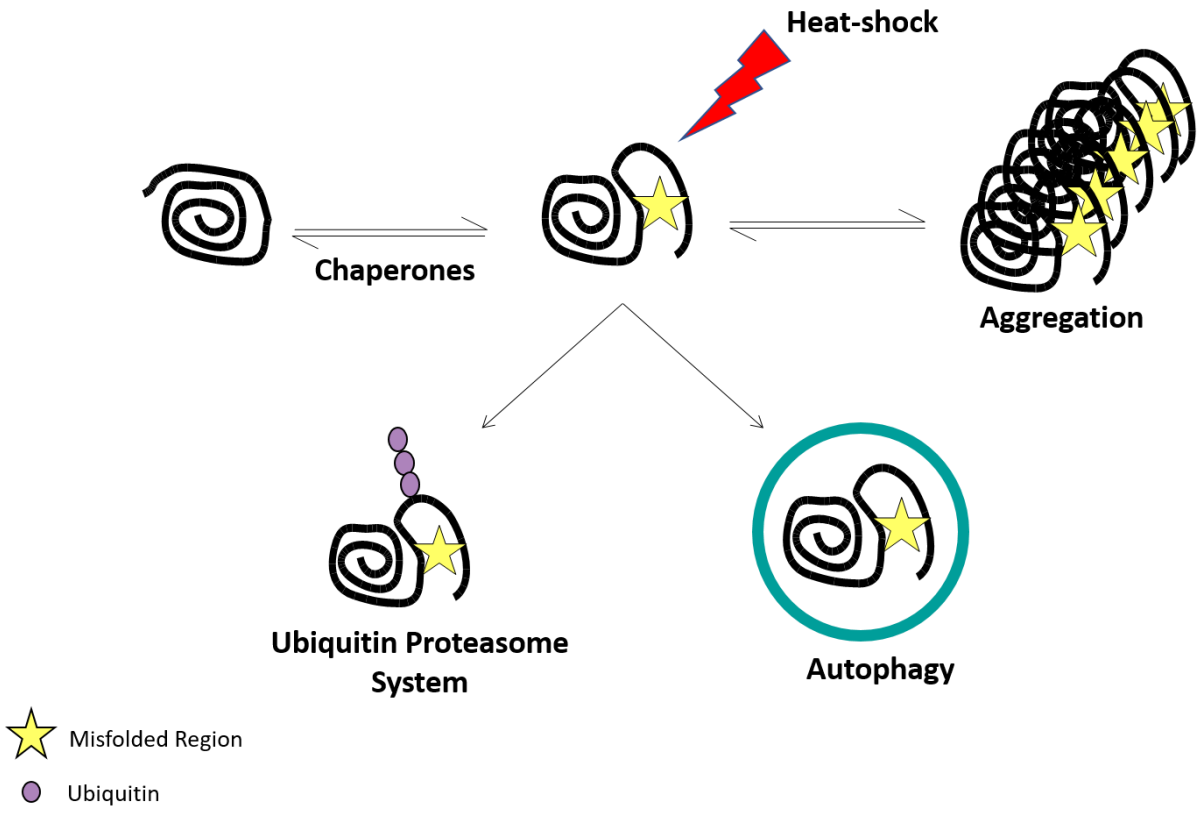

Figure 1.1. Protein Quality Control.

Upon cellular stress like heat-shock, many proteins will misfold. Chaperones attempt to refold and stabilize these misfolded proteins. If they are unable to be folded into a functional state, these proteins must be targeted for degradation through autophagy or the ubiquitin proteasome system. Misfolded proteins that are not refolded or degraded have the propensity to aggregate, which is detrimental to the cell**.**

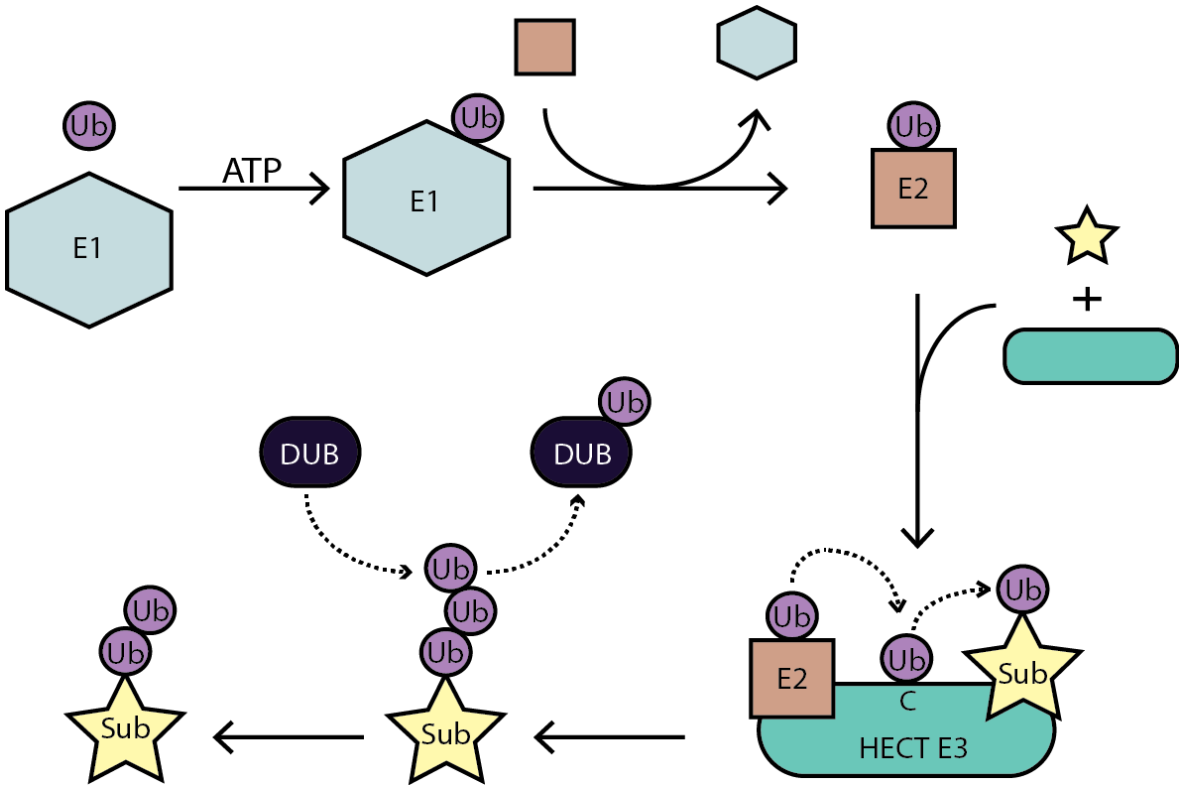

Figure 1.2. The Ubiquitin Cascade.

E1 enzymes activate ubiquitin using ATP by forming a high energy E1~Ub thioester adduct. Once activated, ubiquitin is transferred from the E1 to E2 enzymes. In the case of HECT E3 ligases, the E2s transfer ubiquitin to the catalytic cysteine of E3 ubiquitin ligases where the ubiquitin is then transferred to the substrate. DUBs can also act to remove ubiquitin from the conjugated substrates.

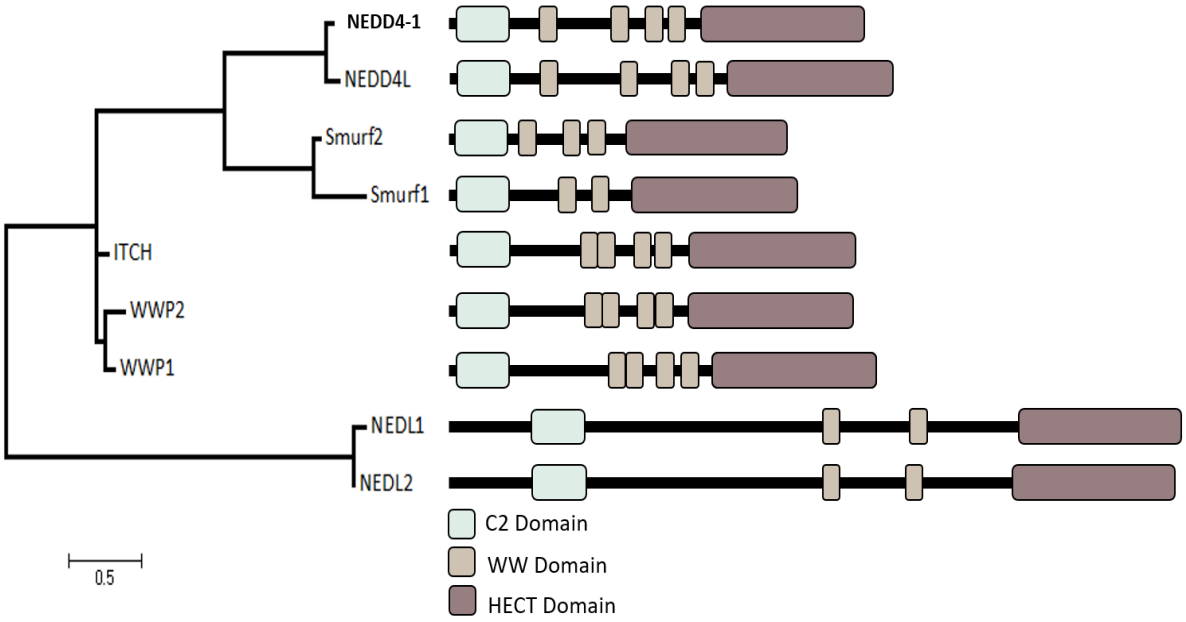

Figure 1.3. Phylogenetic relationship tree of different members of human Nedd4 family E3 ligases based on their HECT domain.

Nedd4-1 clusters with Nedd4L, Itch clusters with WWP1 and WWP2, while Smurf1 and 2, and NEDL1 and 2 form separate clusters. All Nedd4 family E3 ligases have an N-terminal C2 domain, 2-4 WW domains, and a catalytic HECT domain. HECT domain sequences were obtained from Uniprot. This Maximum Likelihood tree was constructed using MEGA software. Scale bar is substitutions per site.

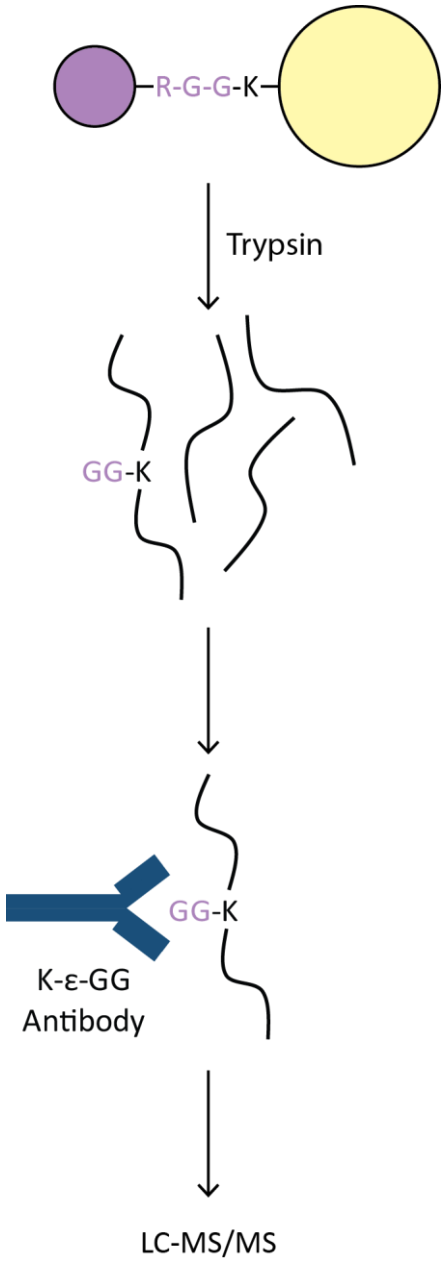

Figure 1.4. Ubiquitin Enrichment Using diGlycine Remnant Antibody for MS Analysis.

Upon trypsin digestion of a ubiquitin-conjugated protein, a signature peptide is produced consisting of the two C-terminal glycines (GlyGly) of ubiquitin that are still covalently attached to the lysine residue of the target protein. As the trypsin is also unable to cleave after the conjugated lysine, this signature peptide contains a mis-cleavage. These peptides can then be enriched using a general motif antibody that only recognizes the K-ε-G-G motif, followed by liquid chromatography coupled with tandem mass spectrometry (LC-MS/MS) analysis.

Chapter 2 - Materials and Methods

2.1. Cell Culture, Cell Lines, and Plasmids

All stable isotope labeling with amino acids in cell culture (SILAC) for the MS experiments were done using human embryonic kidney (Hek293) cells, and Itch KD Hek293 cells (generated from the same cell line). All Nedd4 family member stable shRNA KD cell lines were generated in Hek293 cells. Lentivirus particles were produced using Hek293T cells. Mouse embryonic fibroblast (MEF) wild-type (WT) and MEF Nedd4 -/- cells were provided by Dr. Rotin (SickKids Hospital). The MEF Nedd4 -/- cells were generated as previously described[48]. All SILAC cells were cultured in Dulbecco's Modified Eagle Medium (DMEM) high-glucose SILAC (Caisson Labs, DML07-500ML), 10% dialyzed fetal bovine serum (ThermoFisher, 26400044), 100U/mL streptomycin-penicillin (Invitrogen, 15140122), 73µg/mL lysine (Lys_0, Lys_4, or Lys_8) and 122µg/mL arginine (Arg_0) (all heavy amino acids are from CIL). Stable shRNA knockdown Hek293 cells were maintained in DMEM (Invitrogen, 11965092), 10% fetal bovine serum (FBS) (Invitrogen, 12483020), 100U/mL streptomycin-penicillin (Invitrogen, 15140122), and 0.65µg/mL puromycin (Sigma, P7255). Hek293T cells, HEK293 cells, MEF WT, and MEF Nedd4 -/- cells were maintained as above but without puromycin. shRNA vectors were from Sigma's MISSION human whole-genome shRNA of The RNAi Consortium (TRC) (listed in Appendix 1). Plasmids used for lentivirus particle production were psPAX2 (Addgene plasmid #12259) and pMD2.G (Addgene plasmid # 12259). Plasmid used for addback experiments was pcDNA3.1-V5-ITCH, generated and provided by Dr. Rotin's lab.

2.2. Antibodies

Rabbit polyclonal anti-tubulin antibody (sc-12462, 1:5,000) and mouse monoclonal anti-ubiquitin (sc-53509, 1:5,000) from Santa Cruz were used. Rabbit monoclonal K48-linkage specific polyubiquitin (8081, 1:1,000), rabbit monoclonal K63-linkage specific polyubiquitin (5621, 1:1,000), and rabbit monoclonal anti-hNedd4-1 (3607, 1:1,000) were obtained from Cell Signalling. Mouse monoclonal anti-Itch (611198, 1:1,000) and mouse monoclonal anti-mNedd4-1 (611481, 1:4,000) from BD Biosciences were used. For secondary analysis, the anti-mouse-800, and anti-rabbit-700 fluorescent secondary antibodies (1:10,000; LI-COR) were detected with an Odyssey Infrared Imaging System (LiCor).

2.3. DiGly Peptide Enrichment for HS SILAC Mass Spectrometry Analysis

Only lysine (K) labelling was used for all diGly SILAC experiments. Hek293 cells labelled with light-lysine (K_0) and Hek293 cells labelled with heavy-lysine (K_4) were each grown to 90% confluence in two 15cm plates. Media in all plates was replaced 2 hours prior to the HS experiment. Light-labelled cells were subjected to a 30min HS at 45°C prior to lysis. Cells were washed with PBS, and lysed with 5mL of urea lysis buffer (9M urea, 20mM HEPES pH 8.0, 150mM NaCl, 1mM EDTA, 1mM PMSF, 50mM chloroacetamide, 1mM 1,10-phenanthroline) by scraping and sonication, and then centrifuged at 500*g* for 5min to get rid of cell debris. Equal amounts of heavy- and light-labelled lysate were mixed to obtain 20mg of protein in total. Subsequent enrichment of diGly-containing peptides was performed using the PTMScan Ubiquitin Remnant Motif Kit (Cell Signaling) following the manufacturer's protocol with the following exceptions. Reduction was done using 5mM TCEP, alkylation using 10mM chloroacetamide, and trypsin digestion was done using 200µg TrypZean® bovine recombinant (Sigma, T3568). C18 stage tips were equilibrated with 100% methanol, elution

solvent (0.1% formic acid and 80% acetonitrile), and 0.1% formic acid, before eluting the diGly peptides. An aliquot of total cell lysate (TCL) was also analyzed after stage-tipping[49]. This experiment was done in triplicate, as well as an additional experiment where heavy-labelled cells were heat-shocked instead of the light-labelled cells.

2.4. DiGly Peptide Enrichment for Pulse HS SILAC Mass Spectrometry Analysis

Hek293 cells labelled with medium-lysine (K_4) (control) and Hek293 cells labelled with heavy-lysine (K_8) were each grown to 90% confluence in two 15cm plates. Heavy-labelled media was replaced with light-labelled media (K_0) for 4 hours. These cells were then subjected to a 30min HS at 45°C prior to lysis. Lysis was carried out as previously described. Equal amounts of heavy/light- and medium-labelled lysate were mixed to obtain 20mg of protein in total. DiGly enrichment was carried out as above. An aliquot of total cell lysate (TCL) was also analyzed after stage-tipping. Experiment was done in triplicate, but subsequent MS analysis could only be done on two experiments.

2.5. Mass Spectrometry Analysis

Purified peptides were reconstituted in 1% formic acid with 1% DMSO. Analysis of peptides was carried out on an Orbitrap Fusion Tribrid MS platform (Thermo Scientific). Samples were introduced using an Easy-nLC 1000 system (Thermo Scientific). Columns used for trapping and analytical separations were packed in-house in fritted capillaries prepared using a combination of formamide and Kasil (1:3 ratio). Trapping columns were packed in 100μm internal diameter capillaries to a length of 30mm with C18 core-shell beads (Aeris PEPTIDE XB-C18, Phenomenex, 1.7μm particle size, CAT#04A-4506). After trapping, gradient elution of peptides was performed on a core-shell C18 (Aeris PEPTIDE XB-C18, Phenomenex, 1.7μm

particle size) column packed in 100µm internal diameter capillaries to a length of 25cm and heated to 50°C using AgileSLEEVE column ovens (Analytical Sales & Service). Elution in 60-minute runs was performed with a gradient of mobile phase A (water and 0.1% formic acid) from 3 – 8% B (acetonitrile and 0.1% formic acid) over 2 minutes, 8 – 25% B over 40 minutes, and to 40% B over 11 minutes, with final elution (90% B) using a further 7 minutes at a flow rate of 400nL/min.

Data acquisition on the Orbitrap Fusion (control software version 3.0.2022.16) was carried out using a data-dependent method with MS2 in the ion trap. The Orbitrap Fusion was operated with a positive ion spray voltage of 2200 and a transfer tube temperature of 275°C. MS1 scans were acquired in the Orbitrap at a resolution of 120K, across a mass range of 350 – 1500 m/z, with an RF lens setting of 60, an AGC target of 2e5, a max injection time of 50ms, for 1 microscan in profile mode. For dependent scans, monoisotopic precursor selection was enabled with the 'Peptide' setting, an intensity filter of 5e3, charge state selection of 2 – 4 charges, and dynamic exclusion for 30 seconds after 1 appearance with 20ppm low and high tolerances. Isotopes were excluded from repeat analysis, and the dependent scan on a single charge state per precursor setting was disabled. In MS2 acquisition in the ion trap, quadrupole isolation using a 1m/z window with no offset was used prior to HCD fragmentation with a setting of 32%. Data acquisition was carried out in the ion trap using the 'Rapid' scan rate, a first mass of 110m/z, an AGC target of 1e4, and a max injection time of 30ms for 1 microscan in centroid mode.

TCL peptides were analyzed using a quadrupole – time of flight mass spectrometer (Impact II; Bruker Daltonics) on-line coupled to an Easy nano LC 1000 HPLC (ThermoFisher Scientific)

using a Captive spray nanospray ionization source (Bruker Daltonics) including a 2-cm-long, 100-μm-inner diameter fused silica fritted trap column, 75-μm-inner diameter fused silica analytical column with an integrated spray tip (6 – 8μm-diameter opening, pulled on a P-2000 laser puller from Sutter Instruments). The trap column is packed with 5 μm Aqua C-18 beads (Phenomenex, www.phenomenex.com) while the analytical column is packed with 1.9μm-diameter Reprosil-Pur C-18-AQ beads (Dr. Maisch, www.Dr-Maisch.com). Buffer A consisted of 0.1% aqueous formic acid in water, and buffer B consisted of 0.1% formic acid in acetonitrile. Samples were resuspended in buffer A and loaded with the same buffer. The gradient was run from 0% B to 35% B over 120 min, then to 100% B over 5 min, held at 100% B for 15 min. Before each run the trap column was conditioned with 20μL buffer A, the analytical – with 4μL of the same buffer and the sample loading was set at 20μL. The LC thermostat temperature was set at 7°C. The Captive Spray Tip holder was modified similarly to an already described procedure[50]– the fused silica spray capillary was removed (together with the tubing which holds it) to reduce the dead volume, and the analytical column tip was fitted in the Bruker spray tip holder using a piece of 1/16" x 0.015 PEEK tubing (IDEX), an 1/16" metal two-way connector and a 16-004 Vespel ferrule. The sample was loaded on the trap column at 850 Bar and the analysis was performed at 0.25μL/min flow rate. The Impact II was set to acquire in a data-dependent auto-MS/MS mode with inactive focus fragmenting the 20 most abundant ions (one at the time at 18 Hz rate) after each full-range scan from m/z 200 Th to m/z 2000 Th (at 5 Hz rate). The isolation window for MS/MS was 2 to 3 Th depending on parent ion mass to charge ratio and the collision energy ranged from 23 to 65 eV depending on ion mass and charge[50]. Parent ions were then excluded from MS/MS for the next 0.4 min and reconsidered if their intensity increased more than 5 times. Singly charged

ions were excluded since in ESI mode peptides usually carry multiple charges. Strict active exclusion was applied. Mass accuracy: error of mass measurement is typically within 5 ppm and is not allowed to exceed 10 ppm. The nano ESI source was operated at 1900 V capillary voltage, 0.20 Bar nano buster pressure, 3 L/min drying gas and 150°C drying temperature.

All raw files were subjected to MaxQuant (version 1.5.8.3) for peptide/GlyGly site ID searching against the UniProt human proteome database (March 2017 with 20,123 protein sequences) and peptide quantification. We removed peptides with a C-terminal GlyGly site and peptides that were not detected in all label partners (light, medium, heavy). GlyGly sites with $\log_2 > 1$ were considered to be enriched upon HS and used for subsequent analysis. For each data set, peptide ratios were normalized to the average protein ratio from corresponding TCL aliquots.

2.6. Computational Analyses of Ubiquitinated Substrates Enriched Upon HS

Interaction network of GlyGly sites 2-fold enriched after HS was generated using the STRING application in Cytoscape 3.5.1. Only interactions based on databases (minimum score of 0.9) and experiments (minimum score of 0.4) were considered. Protein localization data was obtained from https://www.proteinatlas.org/ and processed using homebrew Perl (v5.22.1) scripts to extract pertinent data. Data was curated to only contain protein localization information at the 'Supported' level or higher, as detailed on the Protein Atlas website. Data was then clustered into location categories as shown in Table S1. Data was then visualized using the R statistical package (v3.2.3). Protein abundance data was obtained from the https://pax-db.org/ website. Specific sets used were from HEK293 cell lines from the work of Geiger et al. 2012 (9606/485 and 9606/329) and the fill integrated human proteome (9606/29). Data was processed using homebrew Perl (v5.22.1) scripts to match proteins

identified in MS experiments to those contained in the abundance data sets. Data was then visualized using the R statistical package (v3.2.3).

2.7. shRNA KD Stable Cell Line Generation

Ice splinters (50-100 μL) were removed from the frozen bacterial glycerol stock placed into a culture tube containing 0.5mL Terrific Broth without antibiotics. The culture was then incubated at 37°C with shaking (1200rpm) for 25min. 50μL of the incubated culture was then streaked onto Lysogeny broth (LB) agar plates containing 100μg/mL ampicillin, followed by incubation overnight at 37 °C. A single colony was isolated from the plate and used for plasmid DNA preparation using the GenCatch^{TM} Plasmid DNA Midi Prep Kit (Epoch Life Science), following the kit protocol. The day before starting the lentivirus production, a 6cm plate was seeded with $7x10^5$ Hek293T cells in 4mL DMEM with 10% FBS. The following day, 1μg of the purified shRNA was added together with 0.75μg psPAX2, 0.25μg pMD2.G, and up to 20μL of Optimem (Invitrogen, 31985062). This was then added to a second mixture consisting of 74μL Optimem and 6μL FuGENE® 6 Transfection Reagent (Promega, E2691), and then incubated at room temperature for 20min. The complete mixture was added dropwise to the Hek293T cells and incubated overnight. The media of the Hek293T cells was then replaced with 4mL complete DMEM media (containing 10% FBS and 100U/mL streptomycin-penicillin), followed by a 48-hour incubation. The media was removed and filtered through a 0.45μm filter, and then stored at 4°C for no longer than 1 week (media contains lentivirus particles). The day before lentivirus transduction, a 6cm plate was seeded with $2x10^5$ Hek293 cells. The following day, the media was replaced with 3mL lentivirus particle media and 1mL complete DMEM media along with 8μL/mL Polybrene (Sigma, H9268), and incubated

overnight. Media was then replaced with 4mL complete DMEM media and again incubated overnight. The media was then replaced with 4mL complete DMEM media containing 0.65μg/mL puromycin. Cells were maintained and supplemented with fresh media under antibiotic selection every 2 days. Further experiments were not done until cell populations had undergone major cell death and recovery.

2.8. HS Assays in Mammalian Cells

Cells at 80% confluency in 6cm plates were replenished with fresh 4mL media 3 hours before HS, and then transferred to a 45°C incubator for 30min. After HS, cells were washed with PBS and lysed in 200μL of cold modified RIPA buffer (50mM Tris-HCl pH7.5, 150mM NaCl, 1% NP-40, 0.1% SDS, 1mM PMSF, 1× Protease inhibitor cocktail, 50mM chloroacetamide, 1mM 1,10-phenanthroline) by cell scraping and passing through a $27^{1/2}$G needle 10 times on ice. The lysate was then mixed with SDS sample buffer (final 2% SDS) and boiled for 5min at 95°C. Protein concentrations were measured using the DC™ Protein Assay (BioRad, 5000112), followed by western blot analysis. For quantitation using the LiCor Odyssey system, ubiquitination levels were normalized to α-tubulin levels. Significance (p-value) was determined by performing an unpaired student *t*-test (http://www.physics.csbsju.edu).

2.9. HS Solubility Experiments

Cells at 90% confluency in 6cm plates were replenished with fresh 4mL media 3 hours before HS, and then transferred to a 45°C incubator for 30min. Cells were lysed in 200μL following the same protocol as above. Lysates were then spun at 500*g* for 5min at 4°C to remove cell debris, followed by 16,100*g* for 15min at 4°C. Supernatant was removed and mixed with SDS sample buffer (final 2% SDS). Pellets were washed twice with PBS and then resuspended in

100μL of SDS sample buffer (2% SDS). Protein concentrations were measured using the DC™ Protein Assay, and supernatant fractions were normalized to 4mg/mL and pellet fractions were normalized to 0.5mg/mL (due to a much lower concentration). They were then boiled at 95°C for 5min and subsequent western blot analysis.

2.10. Cell Viability Assays

Cells at 70% confluency in 6cm plates (MEF WT and MEF Nedd4-1 -/-) or 3.5cm plates (empty vector control and Itch KD #2) were replenished with fresh 4mL or 2mL media respectively 3 hours before HS, and then transferred to a 45°C incubator for the indicated time. Cells were then washed with PBS, trypsinized until cells detached (2 min at 37°C), and then resuspended in media. For the MEF cells, this suspension was mixed to Trypan Blue at a 1:1 ratio, and followed by automated cell counting using the Countess™ II Automated Cell Counter (ThermoFisher, AMQAX1000), which determined the percentage of living cells in the sample. For the Itch KD experiment, both media and PBS used after the HS were kept and mixed together with the cell suspension prior to mixing with Trypan Blue, due to a large number of cells detaching during the HS. The p-value was obtained by performing an unpaired student *t*-test (http://www.physics.csbsju.edu).

2.11. DiGly Peptide Enrichment for Itch KD HS SILAC Mass Spectrometry Analysis

Empty vector shRNA control cells labelled with medium-lysine (K_4) (control), empty vector shRNA control cells labelled with light-lysine (K_0), and Itch KD #1 cells labelled with heavy-lysine (K_8) were each grown to 90% confluence in 2x15cm plates. Media in all plates was replaced 2 hours prior to the HS experiment. Light- and heavy-labelled cells were subjected to a 30min HS at 45°C prior to lysis. Lysis was carried out as previously described. Equal

amounts of light-, medium-, and heavy-labelled lysate were mixed to obtain 15mg of protein in total. Subsequent diGly enrichment was carried out as above. An aliquot of TCL was also analyzed after stage-tipping.

2.12. Addback Experiments

For Itch addback, 10^6 empty vector control cells and Itch KD #3 cells were seeded in 6cm plates in complete DMEM media. The next day, 5μg of midiprepped pcDNA3.1-V5-ITCH combined with Optimem and FuGENE® 6 Transfection Reagent was added to the cells for 48 hours. HS experiments on these cells were carried out as previously described.

Chapter 3 - Results

3.1. Which Proteins Are Ubiquitinated Upon HS?

To gain a better understanding of the HS ubiquitination response in mammalian cells, we sought to identify which proteins are ubiquitinated upon HS using the diGly enrichment method. Hek293 cells were grown in both light and heavy SILAC media, followed by a 30-minute HS at 45°C of the light labelled cells, while the control heavy labelled cells were maintained at 37°C. Cells were lysed, and equal amounts of each cell lysate were mixed followed by subsequent diGly enrichment and MS processing. We identified 526 GlyGly sites corresponding to 249 proteins. Whereas the diGly modification can be caused by the conjugation of either ubiquitin, Nedd8, or Isg15, it was previously shown that the majority of these sites correspond to ubiquitination events (>95%)[45]. Therefore, diGly sites identified in this study will thereafter be referred to as ubiquitination sites. As expected, the distribution of the SILAC ratios of the ubiquitinated peptides was distinct from the ratios of the proteins in the total cell lysate (TCL) (Figure 3.1A). As well, while only 4% of proteins in the TCL had ratios > $|\log_2 (H/L)|$, about 61% of the GlyGly peptides were more ubiquitinated and 7% were less ubiquitinated (using a two-fold cut off). In parallel, we performed the same experiment but swapped the labelling to heat shock the heavily labelled cells. We identified 228 GlyGly sites corresponding to 165 proteins, and observed a similar shift in the distribution of the SILAC ratios of the GlyGly peptides but in the other direction (Figure 3.1B). As expected, there was an inverse correlation of the ratios of the 148 ubiquitinated peptides quantified in both experiments (Figure 3.1C).

We repeated the experiment two more times to identify and quantify a combined total of 1116 GlyGly sites corresponding to 545 proteins (Figure 3.2A). However, only 116 sites were quantified in all three experiments (Figure A1.A). One possibility is that as the number of ubiquitination peptides in the lysate over capacitated the antibody introducing some variability during the sampling (i.e., immunoprecipitation). Among the 545 proteins identified, 83 were quantified in all three experiments, representing a slightly larger portion. Importantly, the ratio distributions of the quantified ubiquitinated peptides in all 3 replicates show a similar trend (Figure A.1B). The ratio distribution of the ubiquitination sites follows a binomial distribution that differs from the TCL's which follows a normal distribution (Figure A.1B). In total from all 3 replicates combined, there were 657 ubiquitination sites that showed an enrichment upon HS using a two-fold cut off (corresponding to 307 proteins) (Figure 3.2A). We quantified all seven lysine residues of ubiquitin (Figure 3.2B). Interestingly, K27-linked chains showed the greatest enrichment. K48 chains also accumulated, followed by K29 and K63. Intriguingly, while an increase of K63 and K48 polyubiquitin upon HS has been observed before, K29 was not shown to be affected[51]. Commercial antibodies are available for K48 and K63 polyubiquitin chains and confirmed that both linkages increased upon HS (Figure 3.2C).

To obtain a better overview of the data, we created a network based on the physical interaction data using Cytoscape. Among the 307 proteins that were more ubiquitinated, 262 formed a tightly interconnected network (Figure 3.3). There were two clusters of proteins that were apparent: proteins involved in translation (upper left) and proteins involved in RNA processing (upper right). Notably, just under half of the total proteins had only 1 GlyGly site, whereas the rest had multiple, ranging up to 22 sites. Protein localization data was extracted

from Protein Atlas to determine where these HS-dependent ubiquitinated proteins are in the cell. In the TCL derived from the same sample, 33% of proteins are localized with the nucleus, 24% with the cytosol, and 9% with mitochondria (Figure A.2A; Table A.1). In comparison, proteins that are more ubiquitinated after HS display a slightly different distribution with 60% localized to the nucleus, 43% to the cytosol, and 3% to mitochondria (Figure 3.4A). This results in a 1.8-fold increase in nuclear proteins, 1.8-fold increase in cytosolic proteins, and a 3-fold decrease in mitochondrial proteins that are ubiquitinated after HS. In both diGly and TCL samples, there was no dramatic difference in the number of proteins associated with the plasma membrane, endoplasmic reticulum, and cytoskeleton. These results indicate that the majority of proteins getting ubiquitinated after HS are nuclear and cytosolic. We then performed a Gene Ontology (GO) analysis using gProfiler of the proteins ubiquitinated more after HS and found that there was a significant enrichment of proteins involved in messenger RNA (mRNA) metabolic processes, as well as processing of pre-mRNA (Figure 3.4B). Other processes that were enriched among these proteins were RNA transport, SUMOylation, cell cycle, DNA repair, and translation initiation. This correlates with the 2 main clusters that we observed in our interaction network, with the largest being associated with RNA processing. Several proteins involved in mRNA processing are abundant proteins. However, when we compared the protein abundance of the ubiquitinated proteins and proteins identified in their TCL counterparts, we noted that the ubiquitinated proteins that we identified did not necessarily correspond to only abundant proteins (Figure A.2B). By contrast, as it is often the case, the proteins we identified in both experiments (GlyGly and TCL) were in general more abundant. In other words, there was not a true bias towards abundant proteins in our GlyGly enrichment method, but instead the MS itself has a bias for abundant proteins.

Studies in yeast have indicated that newly synthesized proteins are targeted for degradation after HS[14]. It has also been suggested that unstable newly synthesized proteins get ubiquitinated and accumulate when the proteasome is inhibited[52]. We therefore wanted to see what proportion of the ubiquitinated proteins were pre-existing versus newly-synthesized after HS in Hek293 cells. To determine whether the proteins ubiquitinated after HS were recently translated, we used a technique known as "pulse-SILAC". Cells were cultured in heavy-labelled media. The media was then replaced with light-labelled media for 4 hours. This media switch corresponds to $1/9^{th}$ of the doubling time of Hek293 cells cultured in SILAC media (~36 hours). In this context, we referred to proteins that are translated during this time and that are light-labelled as "newly-synthesized". In contrast, heavy-labelled proteins correspond to "pre-existing" proteins. The pulse-SILAC cells were heat-shocked at 45°C for 30 min. In parallel, a control plate with medium-labelled cells was maintained at 37°C (for reference see Figure 3.5A). The two cell populations were lysed and mixed together prior to trypsin digest. A small aliquot corresponding to peptides from the total cell lysate (TCL) was separately analyzed by LC-MS/MS in order to determine the overall ratio of newly translated (light-labelled) vs. pre-existing species (heavy-labelled) for a given protein, as well as to monitor for potential proteins expressed at a different level upon HS. For a given protein that is not affected by HS (due to higher expression or change in turnover rate), the sum of signal intensities in the light and heavy channels should correspond to signal in the medium channel. As expected, among the 4991 quantified peptides a majority do so (91% of peptides have $|\log_2((L+H)/M)| < 1$; Figure 3.5B). The peptides were subjected to a a diGly pulldown to quantify ubiquitination sites. By comparing heavy- and light-to-medium ratios, we identified 537 GlyGly sites, corresponding to 223 proteins, that had been increased after HS (from a total

of 772 sites and 451 proteins) (Figure 3.5B). These modified sites were then subsequently analyzed by their light-to-heavy ratios in comparison to the ratios from their corresponding proteins in the TCL. In this case, we compare a ubiquitinated proteoform to the whole molecule pool of a given protein. Among these ubiquitinated sites, 40% had higher light-to-heavy ratios in comparison to their corresponding ratios in TCL, indicating that these polypeptides ubiquitinated upon HS correspond to newly synthesized proteins (Figure 3.5C). Importantly, the expression of these proteins was not significantly increased upon HS, as the level of light versus heavy SILAC labeling remained low in the TCL. Subsequent GO analysis on the HS-dependent newly-synthesized ubiquitinated proteins showed a significant enrichment of ribosomal proteins, as well as Nucleolar Protein 5A (Nop56p)-associated pre-RNA complex and chaperonin containing TCP-1 (CCT) complex proteins (Figure 3.5D). Surprisingly, the remaining 60% GlyGly sites whose light-to-heavy ratios were smaller than their TCL counterparts correspond to pre-existing proteins ubiquitinated upon HS. There was some enrichment for proteins involved in DNA metabolic processes and negative regulation of cellular organization (Table A4). Overall, there is a large portion of HS-dependent ubiquitinated proteins that are newly-synthesized that are mainly proteins involved in ribosome synthesis and thus impairing translation, whereas pre-existing proteins that are ubiquitinated after HS tend to be DNA associated and involved in transcription.

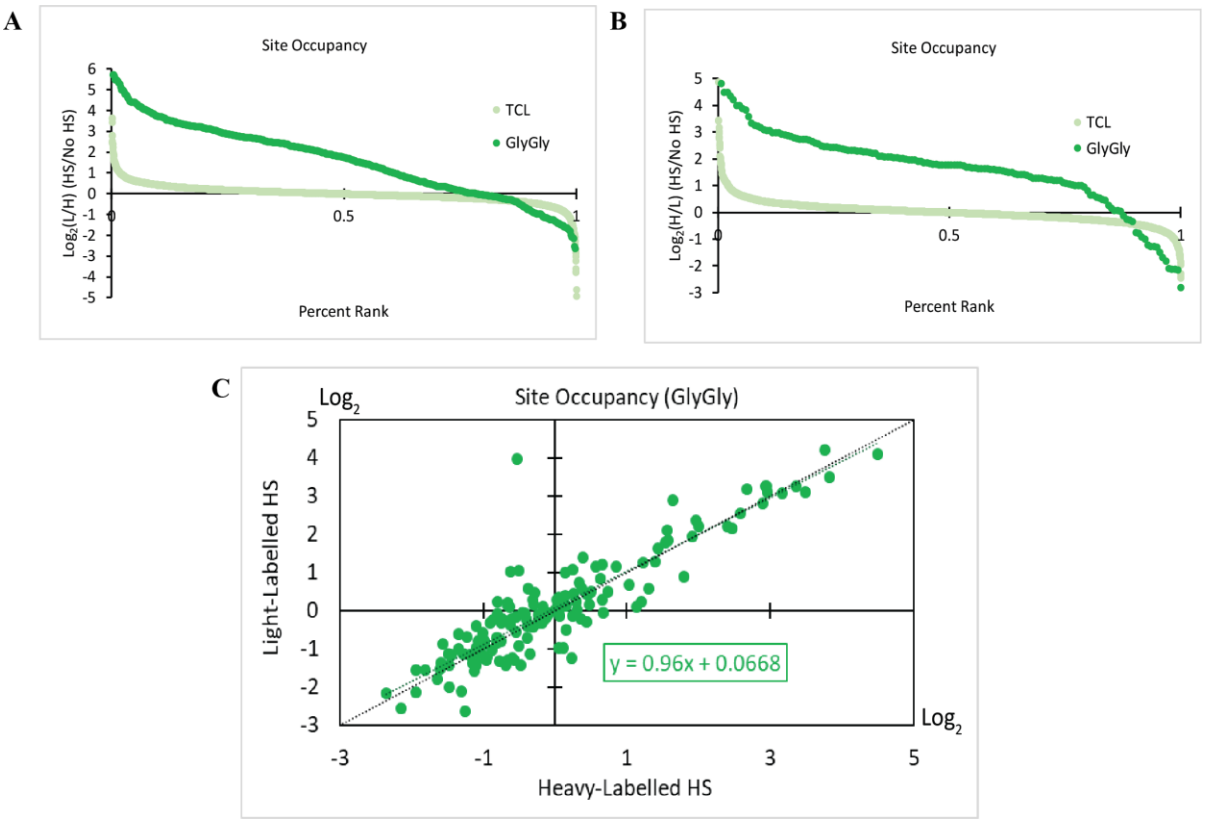

Figure 3.1. Comparing SILAC Labelling for GlyGly Enrichment Upon HS.

(A) Graph of the $\log_2$ ratios of each quantified GlyGly peptide and each quantified peptide from the TCL. In the y axis, combined ratios of heavy (H) versus light (L) are shown to describe the extent of enrichment of each site upon HS. The x-axis reflects where the peptide ranks when the $\log_2$ ratios are organized in descending order. **(B)** Graph of the $\log_2$ ratios of each quantified GlyGly peptide and each quantified peptide from the TCL where the labelling was swapped. Axes are same as in A. **(C)**Plot of the $\log_2$ ratios of the corresponding protein to each quantified GlyGly peptide in the first SILAC HS replicate that was also quantified in the same experiment where the labelling was reversed. The y-axis is the $\log_2$ ratios of the GlyGly sites where HS cells were light-labelled, and the x-axis is the $\log_2$ ratios of the GlyGly sites where HS cells were heavy-labelled. The black line is the expected trend if labelling has no effect on the quantification of HS-dependent diGly sites. The green line is the observed trend.

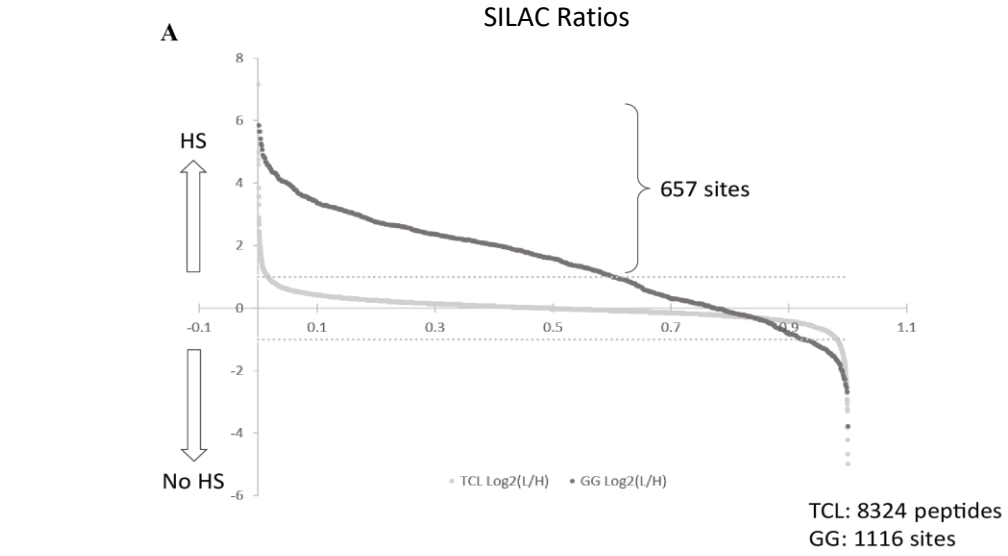

B

Chain Linkage	Fold Enrichment After HS	Intensity
K27	3.3	1.18E+08
K48	2.3	3.37E+09
K29	1.9	94979000
K63	1.5	1.57E+09
K33	1.2	23431000
K11	1.1	7.38E+08
K6	0.8	1.23E+08

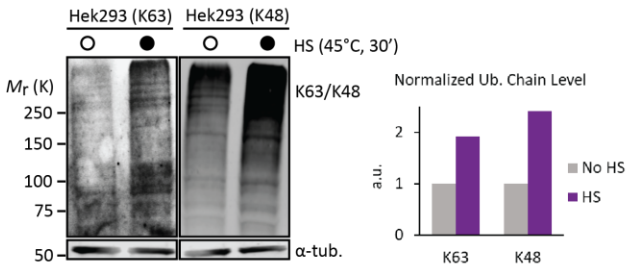

Figure 3.2. GlyGly Site Occupancy of All HS SILAC Replicates.

(A) Graph of the $\log_2$ ratios of each quantified GlyGly peptide in all 3 replicates and each quantified peptide from the TCL from each replicate. In the y axis, combined ratios of heavy (H) versus light (L) are shown to describe the extent of enrichment of each site upon HS. The x-axis reflects where the peptide ranks when the $\log_2$ ratios are organized in descending order. **(B)** Ubiquitin chain specific linkages identified from GlyGly enrichment coupled with LC-MS/MS in 3 replicates. Intensity is the summed up eXtracted Ion Current (XIC) of all isotopic clusters associated with the identified amino acid sequence. **(C)** K63- and K48- ubiquitination levels in Hek293 cells before (open circle) and after HS (black) analysed by western blots (left) and quantified after normalization to α-tubulin (right).

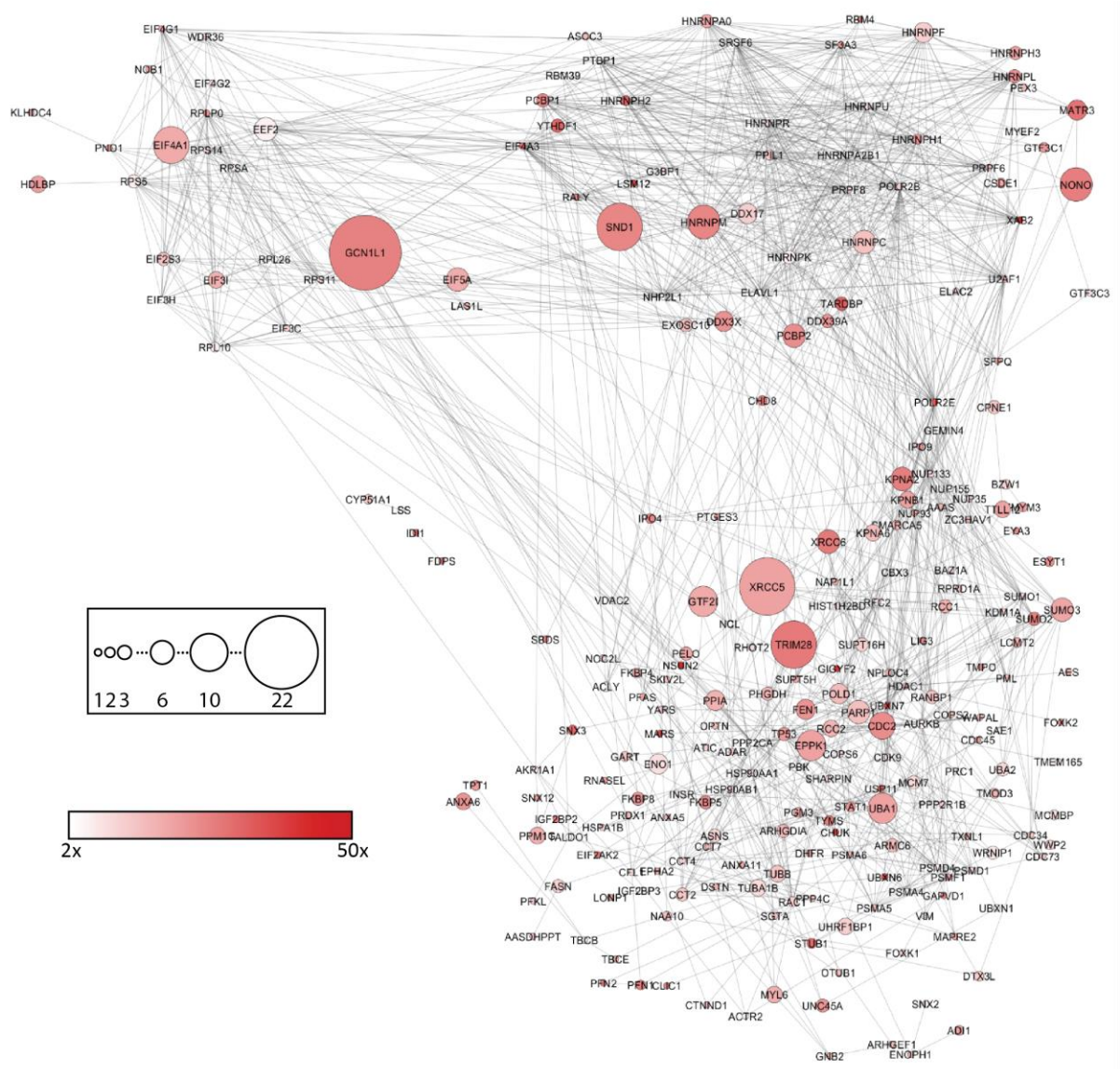

Figure 3.3. Interaction Network of Proteins Ubiquitinated over 2-Fold Upon HS.

The interactions of the 307 ubiquitinated proteins enriched upon HS (from the 3 replicates) were mapped using Cytoscape (see methods). Proteins ranged from a 2-fold enrichment (white) to a 50-fold enrichment (red). Labels are gene names. The size of the node reflects the number of GlyGly sites associated with that protein. Edges are solid lines, indicating a direct interaction based on databases and experiments.

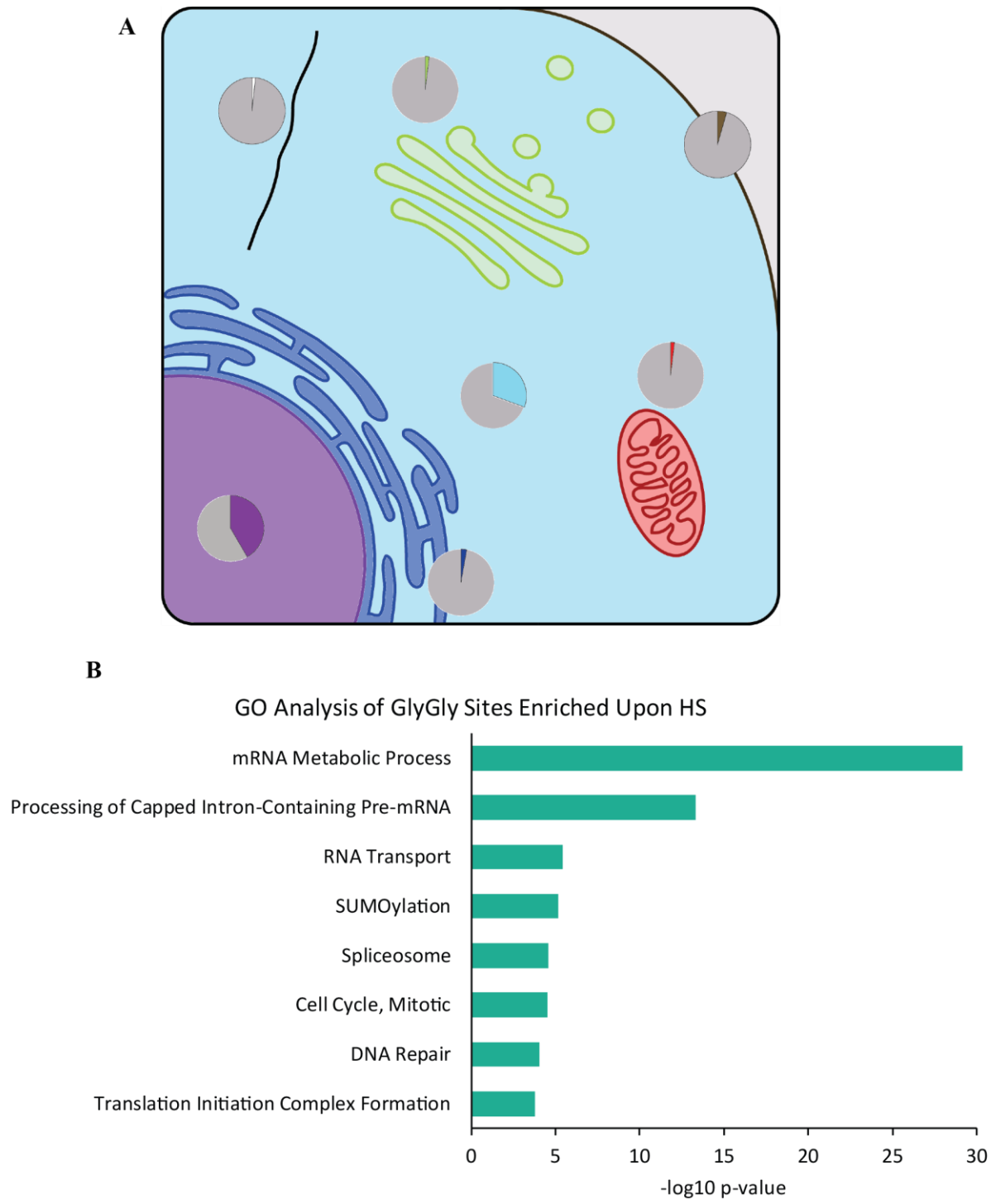

Figure 3.4. Subcellular Localization of Proteins Further Ubiquitinated After HS

(A) Subcellular localization (nucleus = purple, ER = dark blue, cytosol = blue, mitochondria = red, cytoskeleton = black, Golgi = green, plasma membrane = brown). Pie-chart is the proportion of proteins primarily associated with that compartment out of the 324 proteins identified (also summarized in Table A.1). **(B)** GO analysis with gProfiler of proteins that are ubiquitinated more after HS. Significance of enrichment compared to human proteome is shown (-$\log_{10}$ of the p-value) (see also Table A.2).

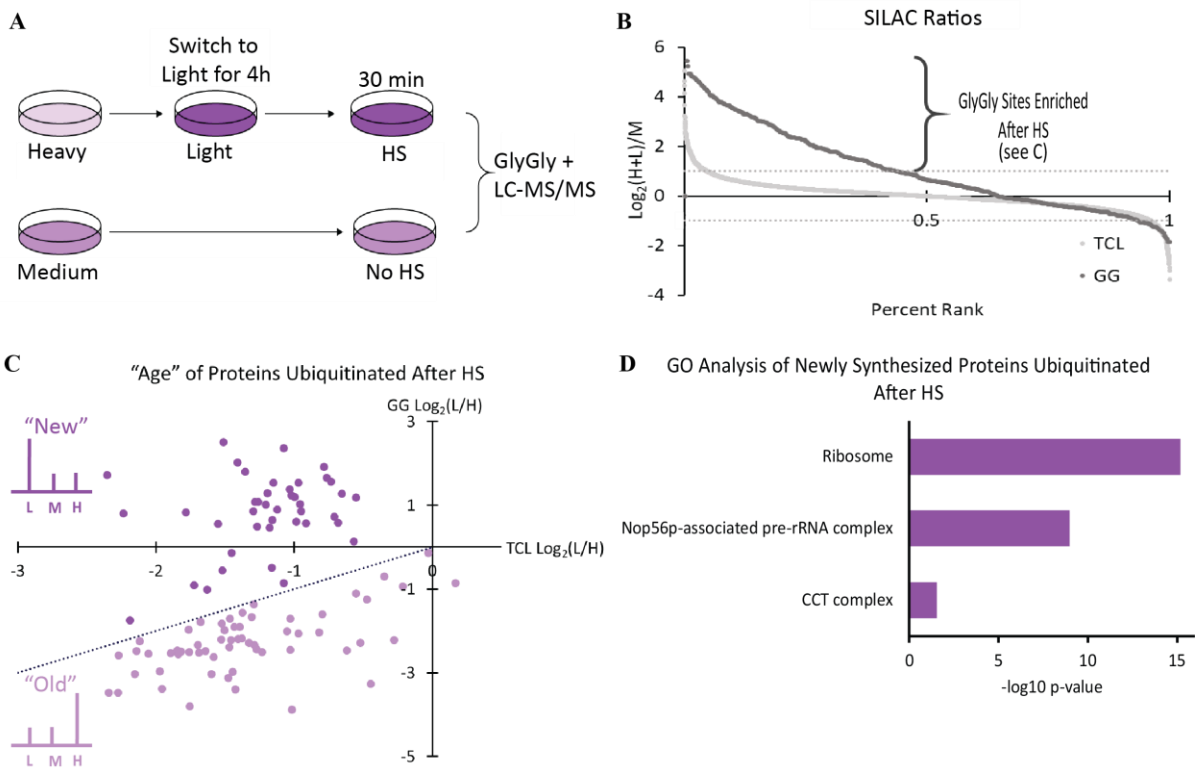

Figure 3.5. HS-Dependent Newly Synthesized Ubiquitinated Proteins.

(A) Schematic of the Pulse SILAC experimental set-up. **(B)** Graph of the $\log_2$ ratios of each quantified GlyGly peptide and each quantified protein from the TCL from 2 experiments. In the y axis, combined ratios of heavy (H) and light (L) versus medium (M) are shown to describe the extent of enrichment of each site upon HS. There are 537 GlyGly sites that had been enriched over 2-fold ($\log_2 > 1$) upon HS. The x-axis reflects where the peptides rank when the $\log_2$ ratios are organized in descending order. **(C)** Plot of the $\log_2$ ratios of the corresponding protein to each enriched GlyGly peptide from (B) that was also quantified in the TCL. If more than 1 site was quantified per protein, the $\log_2$ ratios were averaged. In the y-axis, ratios of H versus of the GlyGly sites (higher ratio indicates newly-synthesized whereas a lower ratio indicates a protein that is long-lived). In the x-axis, ratios of H versus L in the TCL. 40 out of 100 ubiquitinated proteins are newly-synthesized after HS (dark-purple). **(D)** GO analysis with gProfiler of 40 newly synthesized proteins ubiquitinated after HS. $-\log_{10}$ of the p-value of enrichment significance are indicated. (see also Table A.3).

3.2. The Role of Nedd4-1 and Itch in the Hek293 HS Ubiquitination Response.

We had previously shown that Nedd4-1 was required for the increased ubiquitination levels after HS in mammalian cells, but more specifically in MEF and HeLa cells[28]. As our GlyGly experiments were done in Hek293 cells, we sought to address whether Nedd4-1 is also important for the HS response in this cell line.

I transduced Hek293 cells with Nedd4-1 shRNA lentiviruses that target different regions of the mRNA to generate four Nedd4-1 KD stable cell lines (Figure 3.6A). In three cases levels of Nedd4-1 were only moderately reduced (#1, #2 and #4), whereas in the fourth case the KD efficiency was over 80% (#3). As partial KD of Nedd4-1 was sufficient to affect the HS ubiquitination response in HeLa cells[28], I proceeded to evaluate each KD cell line. All four KD cell lines, as well as Hek293 cells which were transduced with an empty vector shRNA as a control, were subjected to a 30-minute HS at 45°C. Ubiquitination levels were then assessed by western blot. Contrary to MEF and HeLa cells, the knock down of Nedd4-1 in Hek293 cells did not have any effect on the ubiquitination levels after HS when compared to the empty vector cells (Figure 3.6B). These results indicate that the reduced levels of Nedd4-1 have no obvious impact on the HS ubiquitination response in these cells.

In our previous studies, we showed that the yeast Rsp5 contributed to the build up of K48 chains after HS in order to promote proteasomal degradation of its substrates[29]. Interestingly, Rsp5 normally synthesizes K63 chains but switches to form K48-linked chains upon HS. Similarly to Rsp5, Nedd4-1 preferentially forms K63-linked chains under normal conditions[53]. Although we did not see the expected decrease in the overall ubiquitination levels

in Hek293 cells upon Nedd4-1 shRNA knockdown, we reasoned that the reduced Nedd4-1 levels could specifically impair the build up of either K63 or K48 chains upon HS. I therefore re-assessed the samples used in Figure 3.4B in which Nedd4-1 was most reduced (#3) using chain specific antibodies. As with ubiquitin, the levels of K63 and K48 chains were both increased upon HS, with no substantial difference between the empty vector control cells and the knockdown cells (Figure 3.7A). These results indicate that the build up of neither K48 nor K63 chains is affected by the reduced levels of Nedd4-1.

It was previously shown that HS mostly leads to the accumulation of poly-ubiquitinated species in the insoluble fraction of the cell after centrifugation[54]. We made the same observations in MEF cells (Figure A.3). We therefore wanted to see if a KD of Nedd4-1 in Hek293 cells had any effect on the ubiquitination of soluble or insoluble proteins. Two KD cells lines and the empty vector cells were again subjected to a 30-minute heat stress at 45°C, and then separated into pellet and supernatant fractions following a centrifugation at 16,100x*g*. Following HS, KD of Nedd4-1 caused a minor reduction of the marked increase of ubiquitination in the pellet fraction where aggregated misfolded proteins accumulate (Figure 3.7B). Similarly, there appears to be a slight depletion of ubiquitin conjugates in the soluble fraction in the KD cells after HS. The same reductions in pellet and soluble fraction was noted when we used the chain specific antibodies. One possibility, is that cell fractionation reduced the signal to noise ratio allowing for better quantitation of the increase in ubiquitination after HS, especially in the pellet fraction. However, these results could not be reproduced in an independent experiment (Figure A.4).

Our results indicate that Nedd4-1 is most likely not the main E3 involved in the HS ubiquitination response in Hek293 cells. Because of its involvement in other cell types, we

thought that perhaps another member of the Nedd4 family could play a more prominent role. As previously mentioned, there are nine Nedd4 family members in *Homo sapiens* (Figure 1.3), and although Nedd4L is most closely related Nedd4-1, other more distant family members have been found to have overlapping roles with Nedd4-1 (see introduction). We therefore decided to investigate the involvement of the eight other ligases in the HS ubiquitination response in Hek293 cells. Using the same method as with Nedd4-1 (shRNA lentivirus), four stable KD cells lines and an empty vector control cell line were generated for each member, apart from NedL2 where only one KD survived. All cell lines were heat shocked at 45°C for 30 minutes whereupon their ubiquitination levels were assessed by western blot. While ubiquitination signals appear to be lower in cells expressing shRNA that target Nedd4L, quantitation showed no consistent decrease of the conjugation levels upon HS (Figure 3.8). Cells expressing Smurf1 and WWP2 targeting shRNA mainly showed no effect on ubiquitination levels (Figure 3.9 and Figure 3.10 respectively). Cells containing shRNA that target Smurf2, WWP1, and NedL2 exhibited a slight increase in overall ubiquitination levels after HS, whereas cells expressing Itch and NedL1 targeting shRNA showed an average decrease in ubiquitination levels (Figure 3.11, Figure 3.12, Figure 3.13, Figure 3.14, Figure 3.15 respectively). To provide a better overview of the results, the averaged changes in ubiquitination levels were graphed together (Figure 3.16). Introducing shRNA targeting both NedL1 and Itch led to lower ubiquitination levels after HS in comparison to controls. However, results from the NedL1 shRNA cells were inconsistent between replicates. I therefore proceeded to further evaluate the role of Itch in the Hek293 HS ubiquitination response.

We showed that KDs of Itch, also known as atrophin interacting protein 4 (AIP4), led to an impaired HS ubiquitination response in Hek293 cells. We repeated the experiment and also

confirmed that Itch levels were reduced in all 4 cell lines (KDs 1-3 showed over 80% KD efficiency) (Figure 3.17). However, there was no correlation between the efficiency of the KD and the impact on ubiquitination levels after HS. To seek confirmation of the involvement of Itch in the HS ubiquitination response, we attempted a rescue experiment by adding back Itch into KD #3 by transient transfection and repeated the same HS experiment. The addback experiment with the wild-type human Itch could be done in this KD because that shRNA targets the 3' untranslated region (UTR) of Itch (Figure 3.17). Despite an over 5-fold overexpression of Itch in the addback cells compared to the empty vector cells, there was no restoration of ubiquitination levels to that of the empty vector cells (Figure A.5). Instead, overexpression of Itch appeared to reduce ubiquitination levels in both unstressed and HS cells, indicating that the overexpression of that ubiquitin ligase may actually have a dominant negative impact.

Despite the fact we could not perform a rescue experiment, we sought to determine whether the reduced levels of ubiquitination after HS upon Itch KD could affect the cell viability during a prolonged stress. Hek293 empty KD control cells and Hek293 Itch KD #2 cells were placed at 45°C for varying time points up to 12 hours. Every 3 hours, cells were trypsinized and mixed with Trypan blue to assess cell viability using an automated cell counter. There was substantial cell detachment throughout the HS and thus all media and washing PBS was kept and mixed with the trypsinized cells before assessing viability, in order to also assess viability of detached cells. There was a dramatic drop of cell viability to below 10% following 6 hours of HS in the KD cells, whereas around 50% of control cells remained viable (Figure 3.18). The control cells instead experienced a dramatic drop in viability in between 9 and 12 hours.

These results indicate that the KD of Itch has some effect on Hek293 cell viability during prolonged HS.

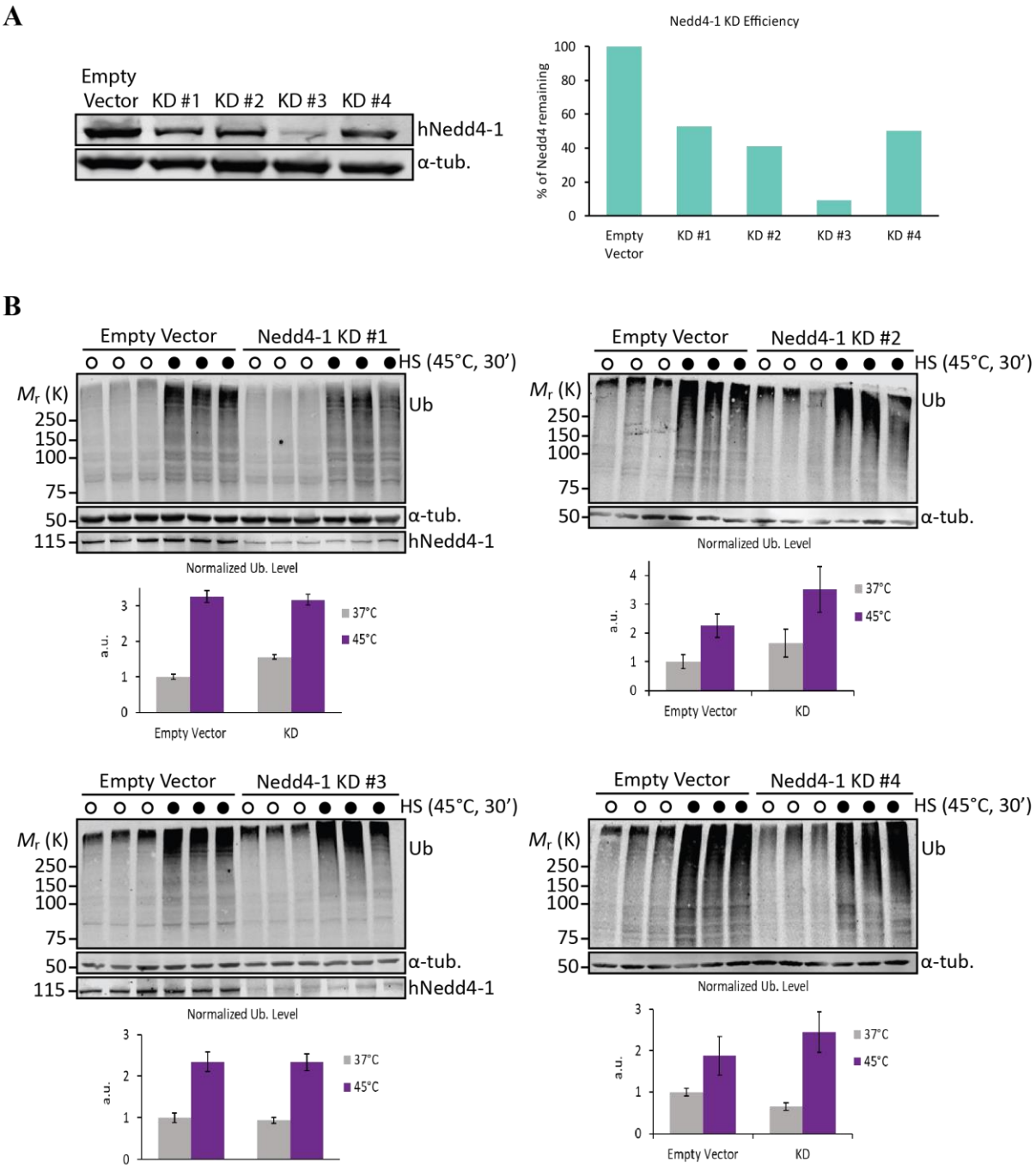

Figure 3.6. Nedd4-1 is not responsible for the increase in ubiquitination upon HS in Hek293 cells.

(A) shRNA KD efficiency in each generated Nedd4-1 KD stable cell line (refer to Table A.5. for more detailed information on each KD clone). Western blot is shown on left and ubiquitin levels normalized to α-tubulin are shown are right. **(B)** Ubiquitination levels in each Nedd4-1 KD cell line compared to an empty shRNA vector control cell line before (open circle) and after HS (black) analysed by western blots (3 biological replicated for each condition). Below each blot is the quantification of ubiquitin levels α-tubulin.

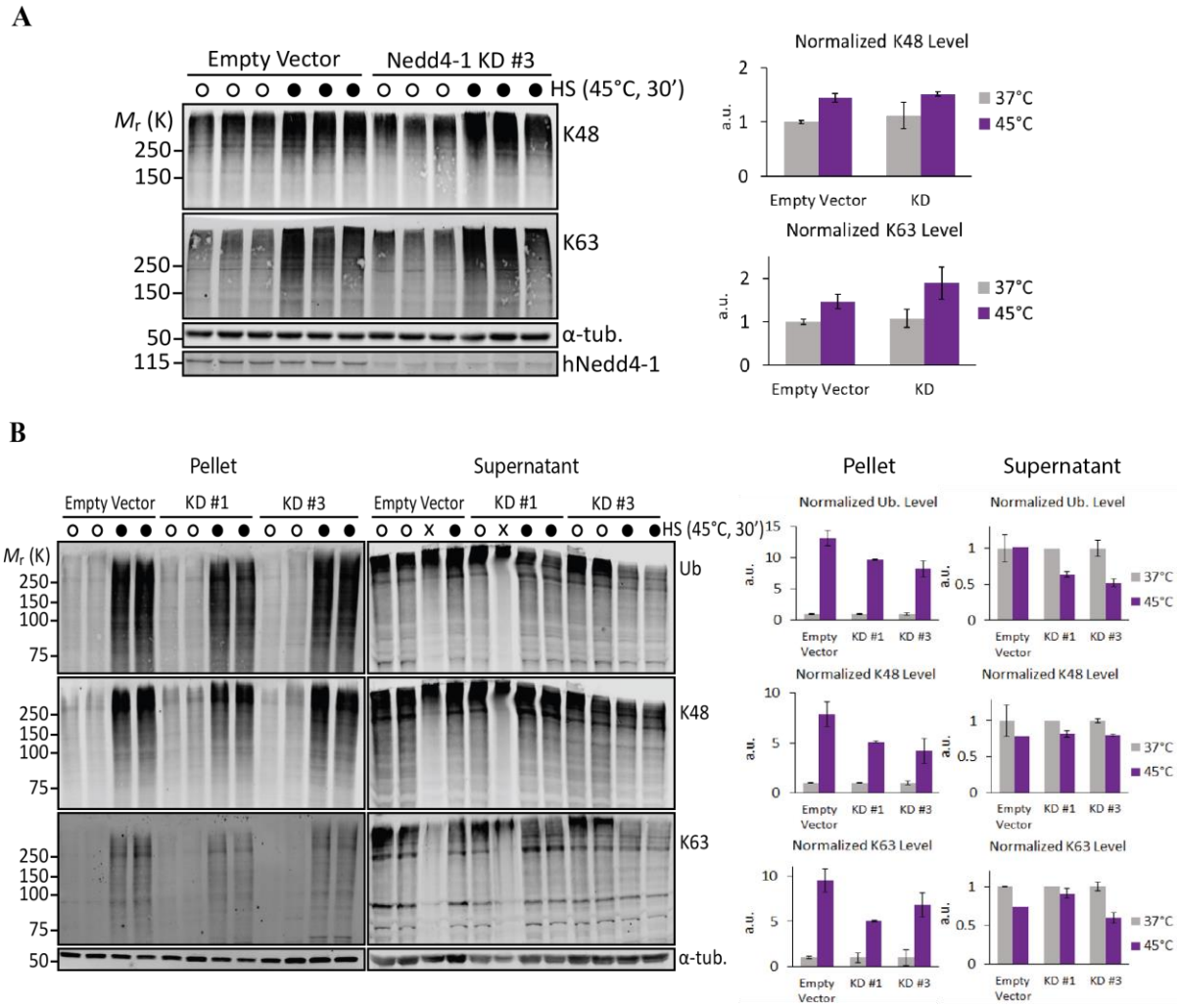

Figure 3.7. Nedd4-1 has no effect on chain linkage specificity but may affect ubiquitination of soluble proteins upon HS.

(A) K48- and K63-ubiquitination levels in Nedd4-1 KD #3 compared to an empty shRNA vector control cell line before (open circle) and after HS (black) analysed by western blots (left) after quantification by normalizing to α-tubulin (right) (3 biological replicates for each condition). **(B)** Total, K48-, and K63-ubiquitination levels of empty vector control cells, Nedd4-1 KD #1, and Nedd4-1 KD #3 cells before and after HS following the separation of each sample into pellet and supernatant fractions (2 biological replicates for each condition; with the exception of a couple samples that were mishandled marked by an "x"). Beside the blot is the quantification of ubiquitin levels normalized to α-tubulin.

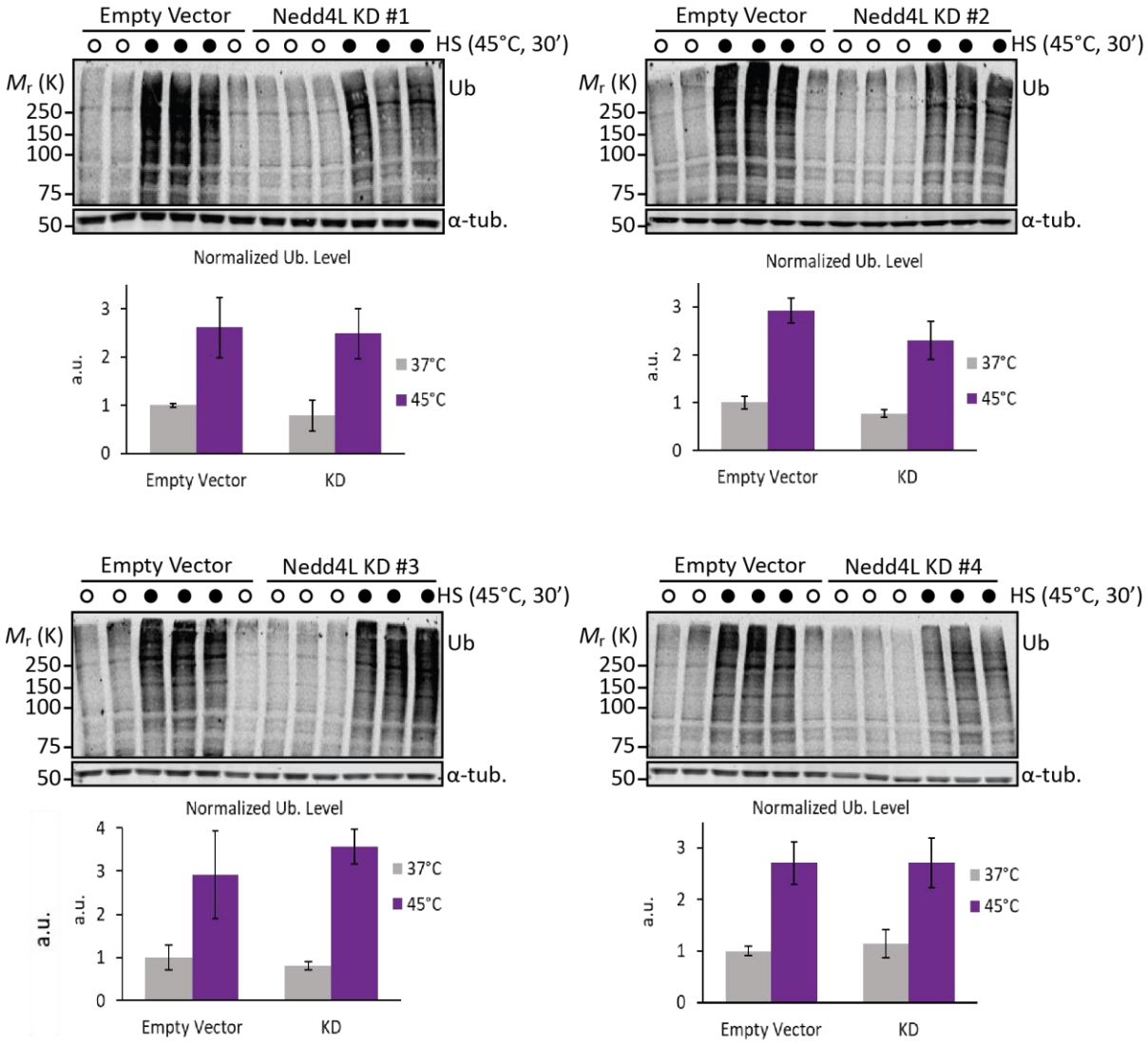

Figure 3.8. Hek293 cells expressing shRNA that target Nedd4L do not affect the ubiquitination levels upon HS.

Ubiquitination levels in each Nedd4L KD cell line compared to an empty shRNA vector control cell line before (open circle) and after HS (black) analysed by western blots (3 biological replicated for each condition). Below each blot is the quantification of ubiquitin levels normalized to α-tubulin.

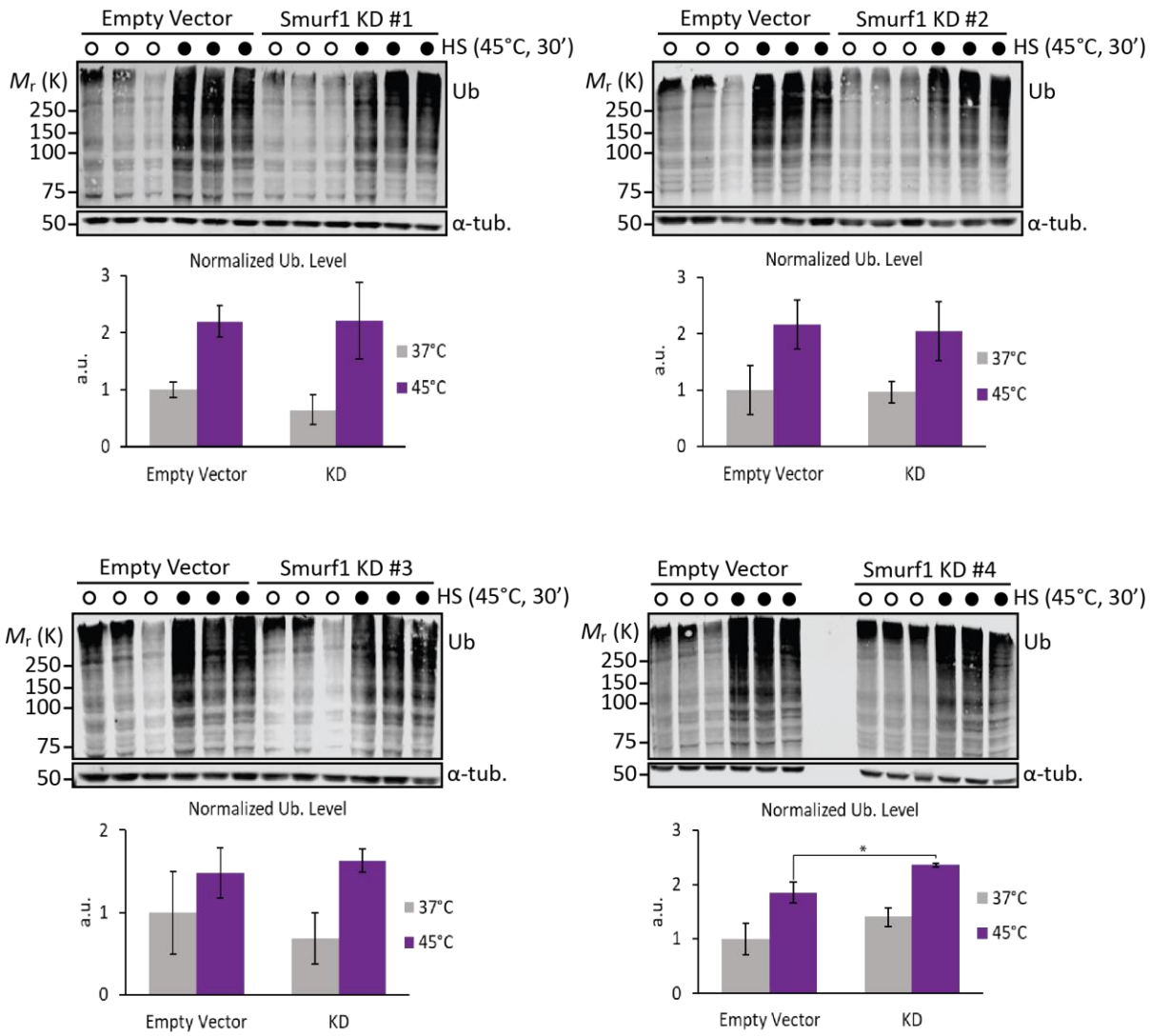

Figure 3.9. Hek293 cells expressing shRNA that target Smurf1 do not affect the ubiquitination levels upon HS.

Ubiquitination levels in each Smurf1 KD cell line compared to an empty shRNA vector control cell line before (open circle) and after HS (black) analysed by western blots (3 biological replicated for each condition). Below each blot is the quantification of ubiquitin levels normalized to α-tubulin. Increased ubiquitination levels were compared using an unpaired student *t*-test (**P*<0.05).

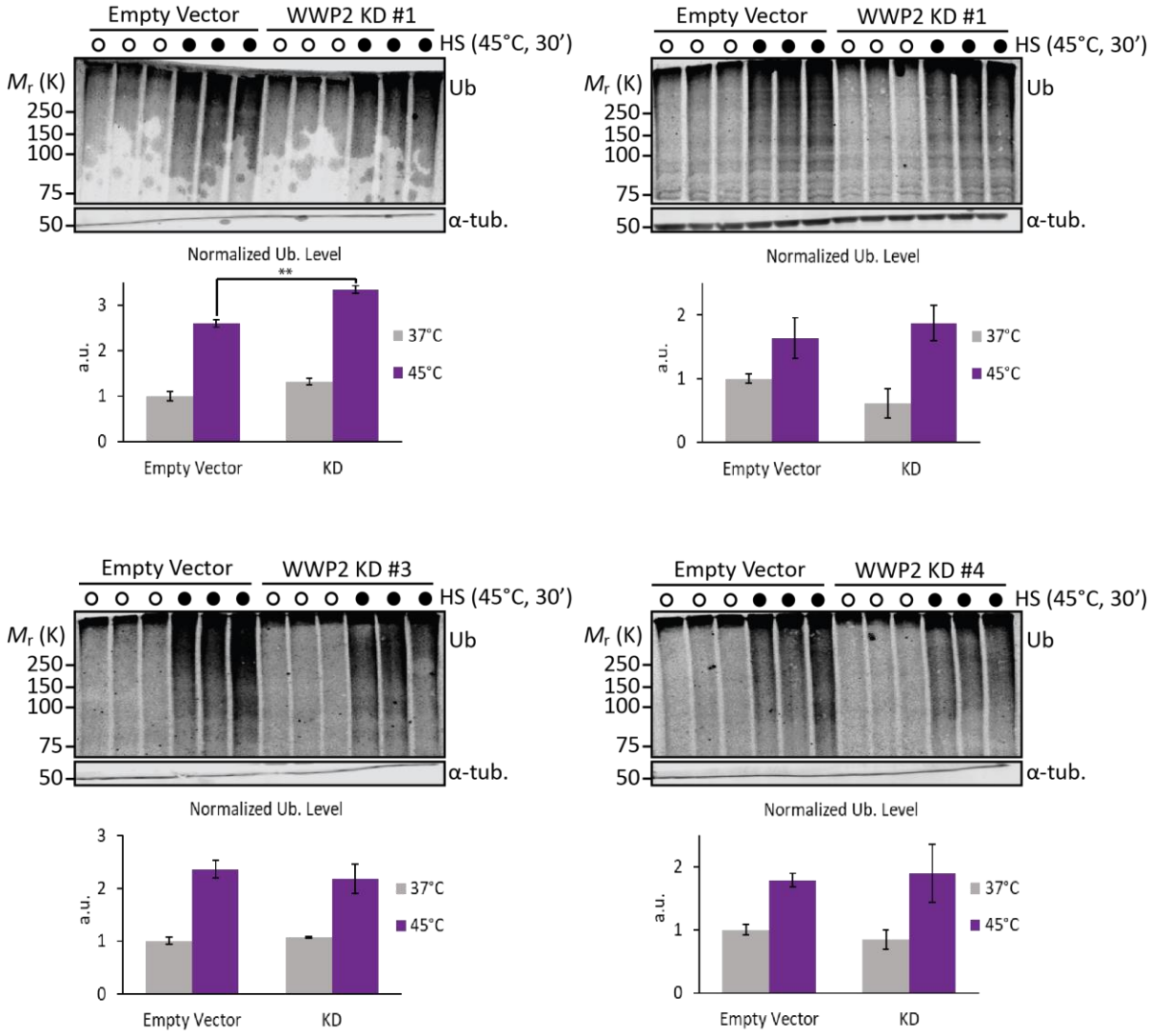

Figure 3.10. Hek293 cells expressing shRNA that target WWP2 do not affect the ubiquitination levels upon HS.

Ubiquitination levels in each WWP2 KD cell line compared to an empty shRNA vector control cell line before (open circle) and after HS (black) analysed by western blots (3 biological replicated for each condition). Below each blot is the quantification of ubiquitin levels normalized to α-tubulin. Increased ubiquitination levels were compared using an unpaired student *t*-test (**P<0.01).

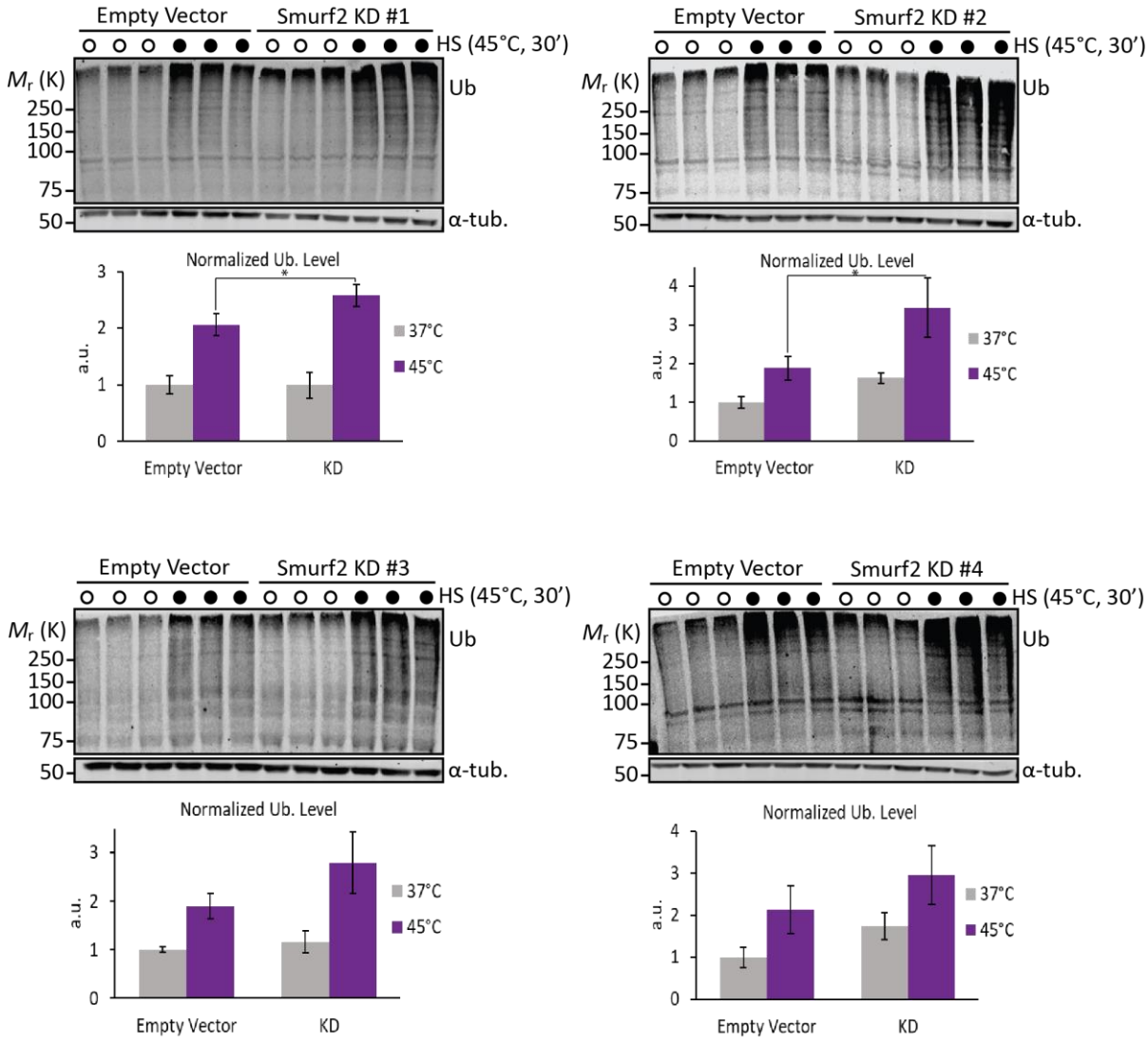

Figure 3.11. Hek293 cells expressing shRNA that target Smurf2 show an increase in ubiquitination levels upon HS.

Ubiquitination levels in each Smurf2 KD cell line compared to an empty shRNA vector control cell line before (open circle) and after HS (black) analysed by western blots (3 biological replicated for each condition). Below each blot is the quantification of ubiquitin levels normalized to α-tubulin. Increased ubiquitination levels were compared using an unpaired student *t*-test (*P<0.05).

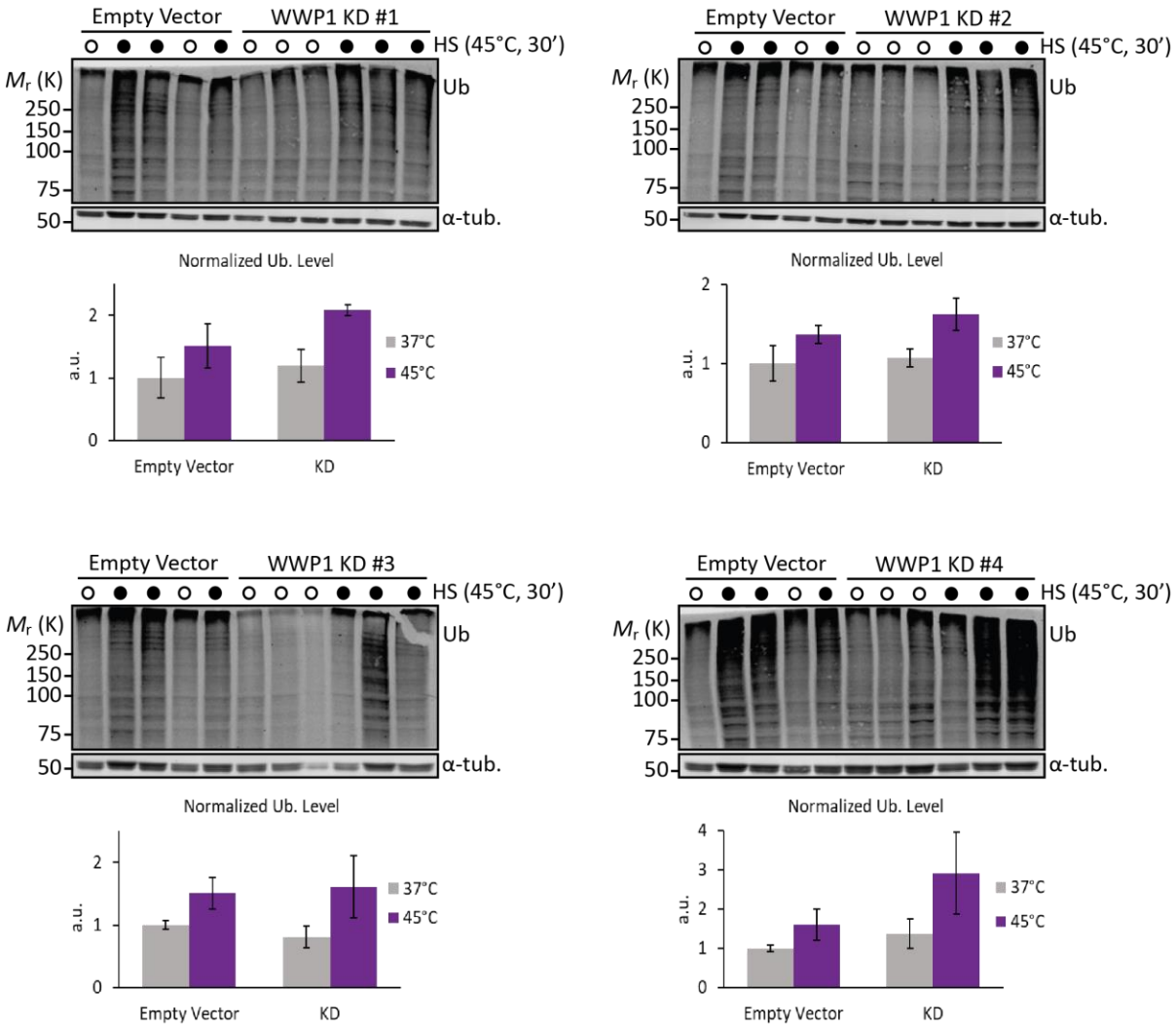

Figure 3.12. Hek293 cells expressing shRNA that target WWP1 show a small increase in ubiquitination levels upon HS.

Ubiquitination levels in each WWP1 KD cell line compared to an empty shRNA vector control cell line before (open circle) and after HS (black) analysed by western blots (3 biological replicated for each condition). Below each blot is the quantification of ubiquitin levels normalized to α-tubulin.

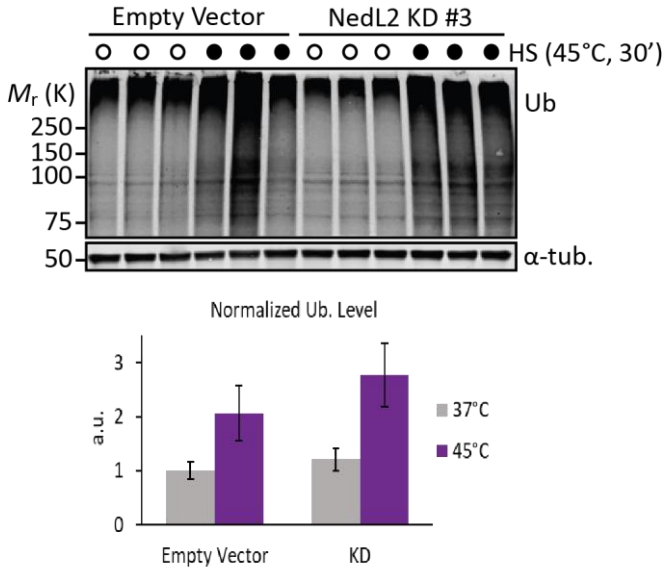

Figure 3.13. Hek293 cells expressing shRNA that target NedL2 show a small increase in ubiquitination levels upon HS.

Ubiquitination levels in a NedL2 KD cell line compared to an empty shRNA vector control cell line before (open circle) and after HS (black) analysed by western blot (3 biological replicated for each condition). Below the blot is the quantification of ubiquitin levels normalized to α-tubulin.

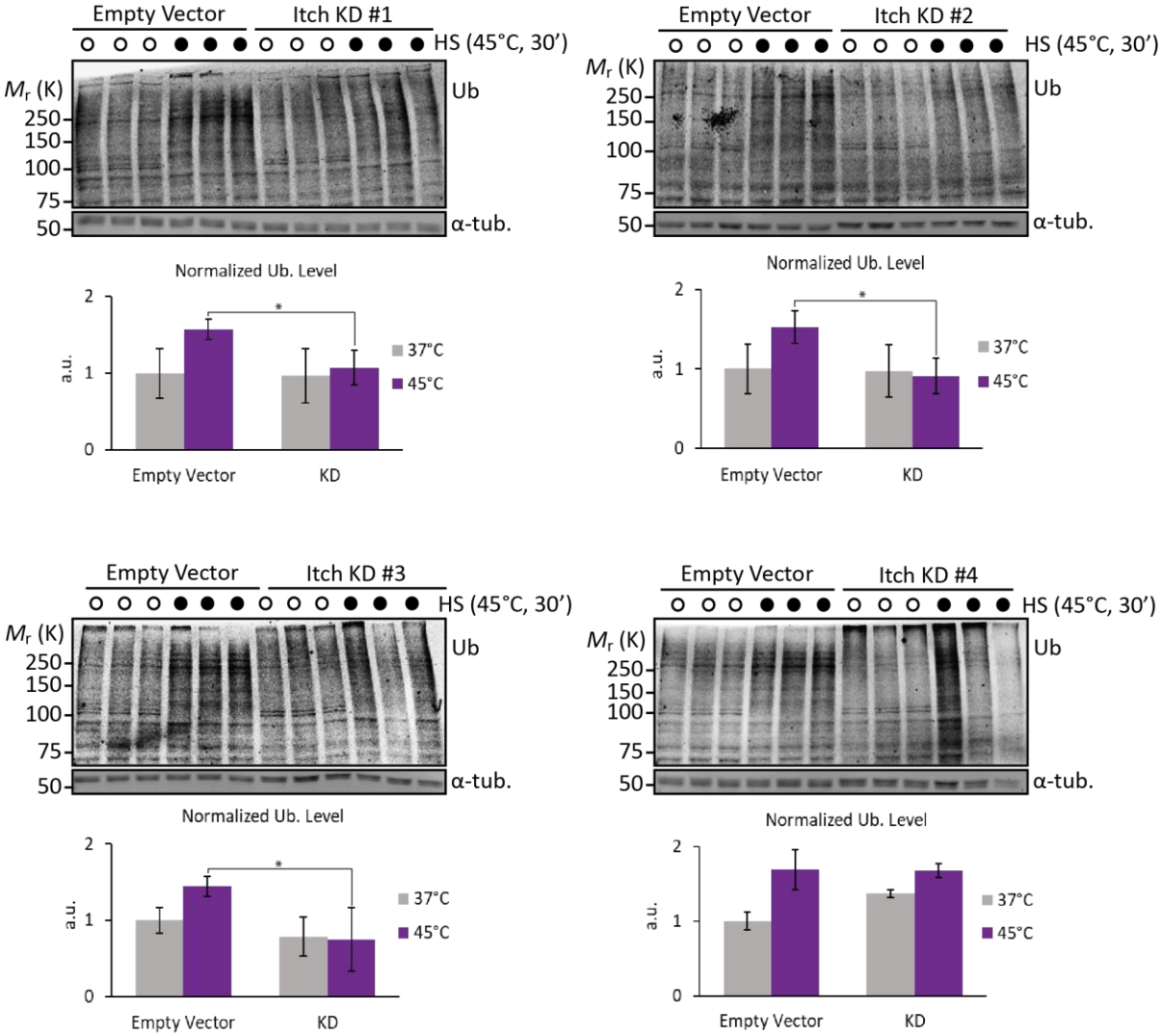

Figure 3.14. Hek293 cells expressing shRNA that target Itch show a significant decrease in ubiquitination levels upon HS.

Ubiquitination levels in each Itch KD cell line compared to an empty shRNA vector control cell line before (open circle) and after HS (black) analysed by western blots (3 biological replicated for each condition). Below each blot is the quantification of ubiquitin levels normalized to α-tubulin. Increased ubiquitination levels were compared using an unpaired student *t*-test (**P*<0.05).

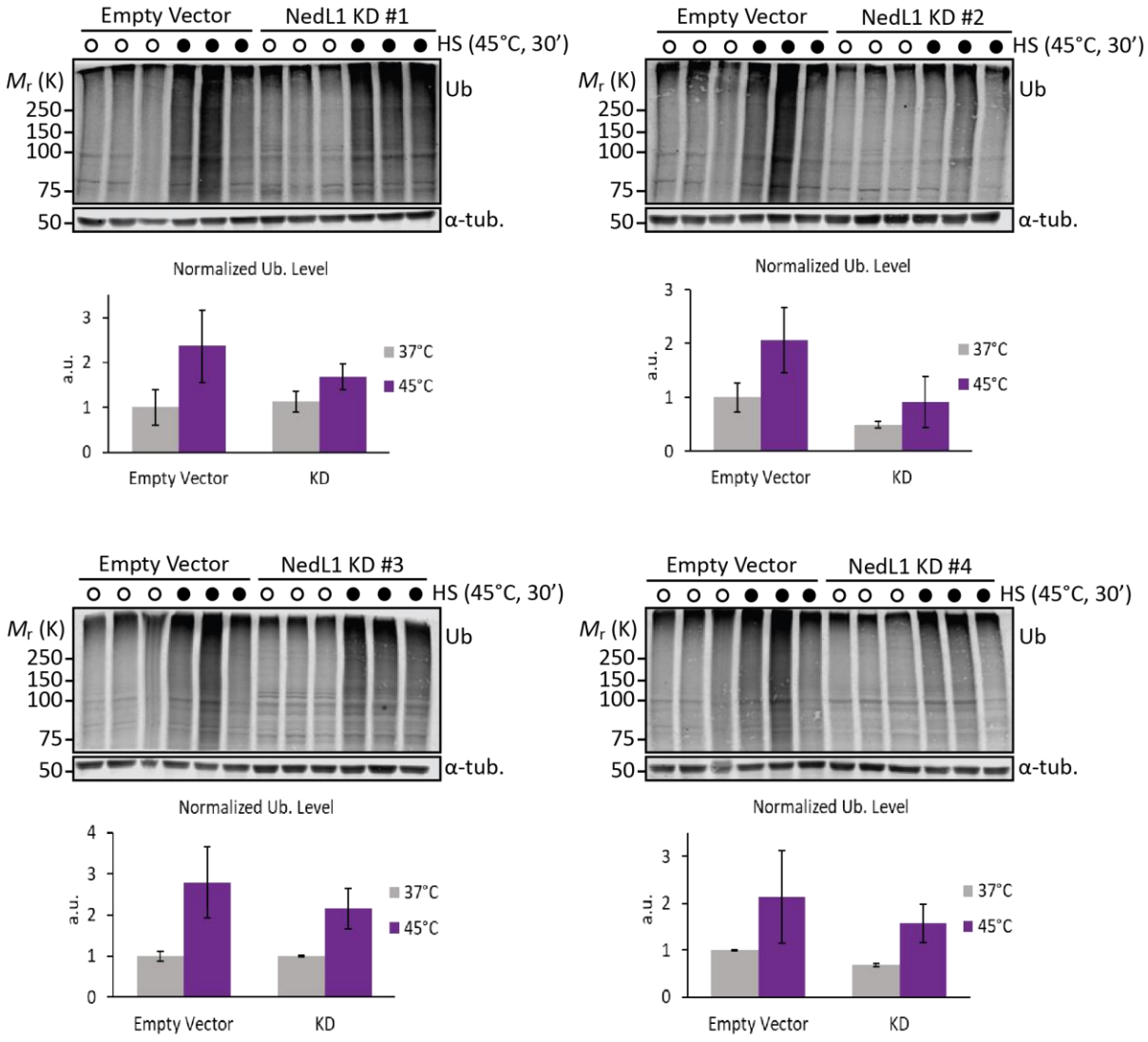

Figure 3.15. Hek293 cells expressing shRNA that target NedL1 show a decrease in ubiquitination levels upon HS.

Ubiquitination levels in each NedL1 KD cell line compared to an empty shRNA vector control cell line before (open circle) and after HS (black) analysed by western blots (3 biological replicated for each condition). Below each blot is the quantification of ubiquitin levels normalized to α-tubulin.

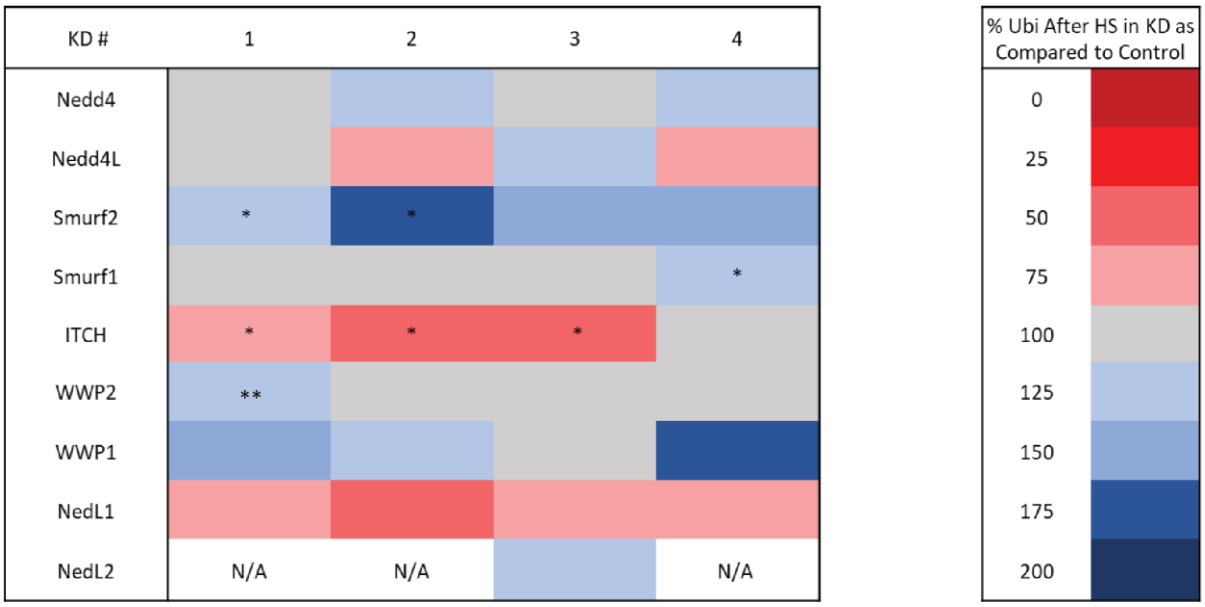

Figure 3.16. Summary of the Role of Nedd4 Family Members in the HS Ubiquitination Response.

Comparison of ubiquitination levels after HS in each clone as compared to levels in the empty vector control cells (as a percentage). Grey represents no change in ubiquitination (100%), dark blue represents that there is twice as much ubiquitination in the KD cells (200%), and dark red represents that there is no ubiquitination occurring in the KD cells after HS (0%). KDs that exhibit significant differences in ubiquitination after HS from the control cells are indicated by an asterisk (*p-value < 0.05, **p-value<0.01).

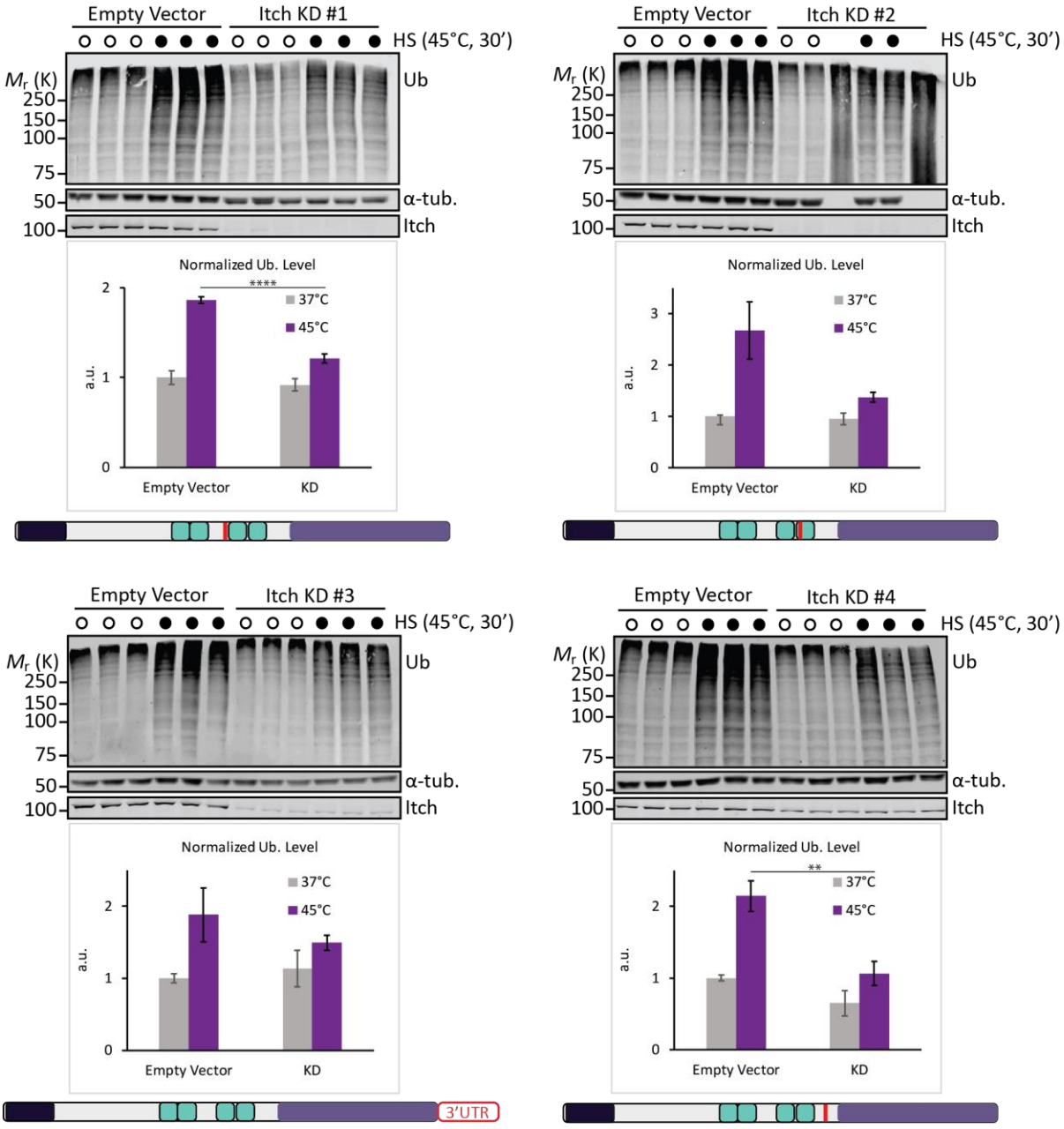

Figure 3.17. Confirmation of the effect of Itch KD on the HS ubiquitination response.

Second experiment where ubiquitination levels in each Itch KD cell line compared to an empty vector control cell line before (open circle) and after HS (black) analysed by western blots and normalized to α-tubulin (3 biological replicated for each condition). Below each blot is the quantification of ubiquitin levels normalized to tubulin. Below each KD is a representation of the Itch protein sequence indicating where the shRNA is targeting (red). Increased ubiquitination levels were compared using an unpaired student *t*-test (***P*<0.01, *****P*<0.0001).

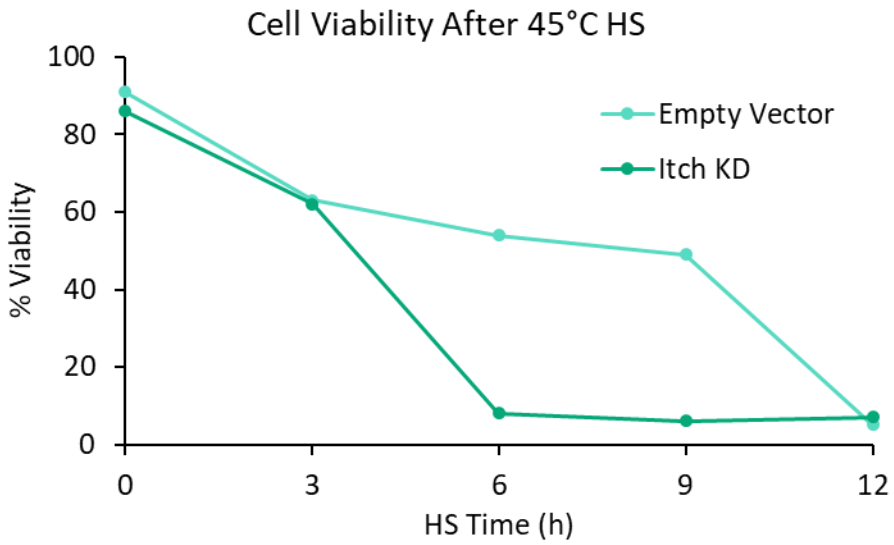

Figure 3.18. Effect of Itch KD on cell viability.

(A) Graph of the cell viability of empty vector control cells and Itch KD #2 cells after HS of the indicated time. Viability percentage indicates the number of cells that are still alive from the total cell pool as determined by Trypan Blue staining and automated cell counting.

3.3. Confirming the Role of Nedd4-1 in the MEF HS Ubiquitination Response.

Our previous efforts to investigate the mammalian heat-shock ubiquitination response identified Nedd4-1 as the main E3 in MEF cells that is responsible for an increase in ubiquitination levels upon heat-shock[28]. Our results in Hek293 cells, in which Itch seems to be the main ubiquitin-ligase involved in this response, were therefore surprising. One possibility is that the growth conditions could alter which HECT ligase from the Nedd4 family plays a major role during the stress response. Consequently, we wanted to verify our previous results with MEF cells and further characterize the HS response in these cells.

MEF Nedd4-1 +/+ (denoted WT) and Nedd4-1 -/- (denoted KO) cells, which were generously provided by D. Rotin, were subjected to a 45°C heat stress for 30 min. Ubiquitination levels were then assessed by western blot. As shown previously, we found that ubiquitination levels after heat-shock in the KO cells were dramatically lower in comparison to the control WT cells (Figure 3.19A). Although the difference with WT cells was significant, there was still a small increase in ubiquitination in the KO cells. The results indicate that, besides Nedd4, another E3 ligase may also be involved in targeting proteins after HS in MEF Nedd4-1 -/- cells.

We next wanted to assess which poly-ubiquitin chain linkages accumulated in the MEF cells upon HS. We reasoned that since Nedd4 may play a major role in the HS response in these cells, different chain linkages may be assembled in contrast to Hek293 cells. We therefore reanalyzed our samples by western blot using antibodies specific to K63 and K48-chains. In the WT cells, both chains showed over a 2-fold increase in polyubiquitin levels (Figure 3.19B). These results are similar with our previous work in Hek293 cells. In contrast,

our published work in yeast showed a more prominent accumulation of K48-linked chains that were assembled by Rsp5 upon HS, while a less prominent accumulation of K63-linked chains that were assembled by Hul5[29,55]. Levels of both K63 and K48-linked chains remained low upon HS in the Nedd4 -/- cells compared to the control cells (Figure 3.19B). These results reinforce that Nedd4-1 does play a role in the HS-induced ubiquitination response in MEF cells.

To further illustrate the importance of the increased in ubiquitination upon HS, we wanted to determine whether the loss of Nedd4-1 in MEF cells affects cell survival under this stress. We reasoned that the absence of Nedd4-1 in MEF cells could cause a reduced cell viability, as these cells may not be able to appropriately clear misfolded proteins. MEF WT and MEF Nedd4-1 -/- cells were placed at 45°C for 2 hours. After the 2-hour HS, cells were trypsinized and mixed with Trypan blue to assess cell viability using an automated cell counter. After heat-shock, 35% of WT cells remained viable, whereas only 10% of -/- cells were still alive (Figure 3.19C). These results indicate that there is a significant loss of cell viability upon HS in MEF cells lacking Nedd4-1.

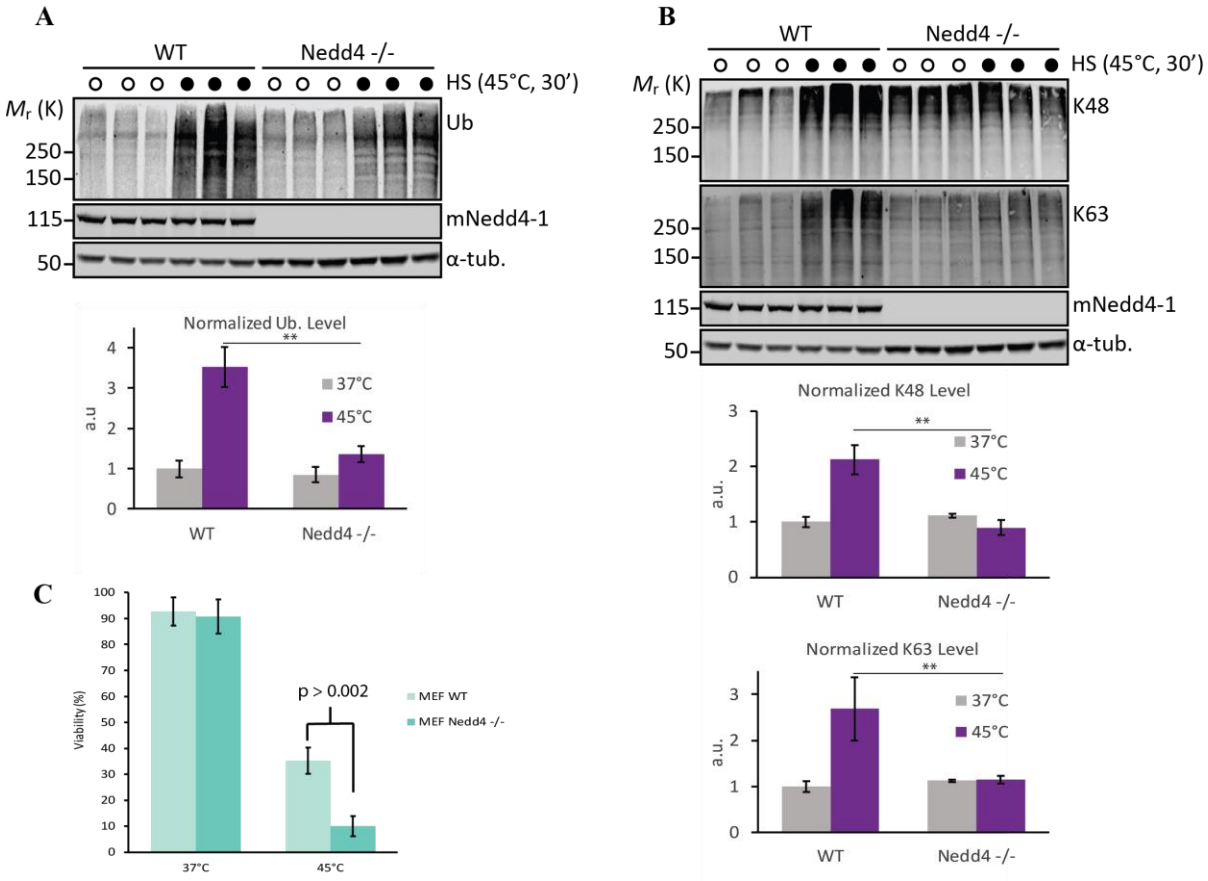

Figure 3.19. The Role of Nedd4-1 in the HS ubiquitination response in MEFs.

(A) Ubiquitination levels in MEF Nedd4 -/- cells compared to WT cells before (open circle) and after HS (black) analysed by western blots and normalized to α-tubulin (3 biological replicated for each condition). Increased ubiquitination levels were compared using an unpaired student *t*-test (***P*<0.01). **(B)** K48- and K63-ubiquitination levels in MEF Nedd4 -/- cells compared to WT cells before and after HS analysed by western blots and normalized to α-tubulin (3 biological replicated for each condition). Increased chain linkage levels were compared using an unpaired student *t*-test (***P*<0.01). **(C)** Bar graph of the cell viability of MEF WT and MEF Nedd4 -/- cells after a 2-hour HS from 4 independent experiments. Viability percentage indicates the number of cells that are still alive from the total cell pool as determined by Trypan Blue staining and automated cell counting. Difference in viability is significant (p-value < 0.0022).

Chapter 4 - Discussion

4.1. Which Proteins Are Ubiquitinated Upon HS?

Using the GlyGly enrichment method coupled with LC-MS/MS, we identified 307 proteins that were ubiquitinated upon HS. Several ubiquitin chain linkages accumulated after HS, especially K27 and K48, whereas K6, K11 and K33 remained unchanged. Although K48 is a known marker for proteasomal degradation, and thus its increase upon HS directly correlates to the greater need for protein degradation, K27 is not as widely studied. It has recently been found however that histones H2A/H2A.X can be ubiquitinated by K27-linked chains and that this is strictly required to activate the DNA damage response[56]. Heat stress causes double stranded breaks during the G1 and G2 phases, as well as an arrest in the progression of the replication fork which often causes an accumulation of single stranded breaks[57,58]. This HS dependent enrichment of K27 chains could possibly be activating the DNA damage response due to the DNA damaged incurred upon HS. This result could also coincide with an enrichment of ubiquitinated DNA repair proteins in our experiments such as DNA Ligase 3 (LIG3), X-ray repair cross-complementing protein 5 (XRCC5), and Poly [ADP-ribose] polymerase 1 (PARP1). It should be noted however that although K-27 ubiquitination was shown to be associated to H2A/H2A.X, H2A showed minimal change in its ubiquitination after HS and ubiquitination of H2A.X showed over a 2-fold depletion upon HS in our data set which is in accordance with other work[59]. It is therefore plausible that K27 polyubiquitination could be more prominently conjugated to other DNA repair proteins instead of histones during the HS response. Interestingly, UBR4/5 has recently been shown to produce K11-K48 branched chains, which were shown to be proteasomal priority signals and allow cells to rapidly clear aggregation-prone proteins[60]. It is therefore surprising that K11 chains do not

accumulate upon HS in our experiments and suggest that UBR4/5 may not contribute the ubiquitination after HS (see also below for an alternative explanation).

A large portion of proteins ubiquitinated after HS in tissue culture cells are cytosolic, which is similar to what we found in yeast cells[55]. These results indicate that there is an overall conservation of the HS response from yeast to mammals. In addition, there was an enrichment of nuclear proteins and mitochondrial proteins were under-represented as compared to the proteome analysis of the TCL fraction. This loss of mitochondria associated ubiquitinated proteins upon HS could simply be due to there being no access to ubiquitin within mitochondria. It has also been recently shown that reduced mitochondrial activity has been linked to an increase in stress resistance as well as cytosolic proteostasis upon HS[61]. The increase in ubiquitinated nuclear proteins can be related to some of the pathways and processes affected upon HS. After performing a GO analysis on this GlyGly list, there was a significant enrichment of proteins involved in mRNA metabolic processes, and more specifically, pre-mRNA processing (splicing) and RNA transport. It has been reported that under heat stress in mouse fibroblasts, especially severe HS like in our experiments, nearly 2000 genes have inhibited splicing and that these intron-containing transcripts are largely nuclear and untranslated[8]. The ubiquitination of the machinery involved in intron splicing and the transport of the mRNA out of the nucleus that we observed in our experiments could possibly inhibit these processes by either targeting them for degradation or sequestering them in the nucleus until they are needed for when the cell is no longer stressed.

Additionally, in our GO analysis, there was a significant enrichment for proteins involved in SUMOylation. It is known that SUMO-2 and SUMO-3 are required for cell survival after HS, and that ubiquitination can occur on the same residues as SUMOylation[39,62].

SUMO2-K63 hybrid chains have also been shown to exist and play a role in DNA damage, which similarly to K27, could explain why HS-dependent ubiquitinated SUMO-2 was found in our experiments[63]. We cannot therefore discount the possibility the existence of other types of hybrid SUMO-ubiquitin chains that help maintain cellular proteostasis under HS conditions. For example, using a lysine deficient SUMO strategy combined with proteomics, it was found that K63 ubiquitin is predominantly SUMOylated under normal conditions, whereas K11 is SUMOylated under heat stress[64]. K11-chains are known to target cell cycle factors for proteasomal degradation[17]. These findings could be supported by the fact that we found an enrichment for cell cycle proteins upon GO analysis. As we previously discussed however we found no evidence of an increase in K11 chains upon HS. It is possible that although there may be an increase in some K11 chain associated pathways, there may also be a decrease in other K11 pathways that are Ubr4/5 dependent, causing net unchanged levels upon HS.

It has been suggested that between 6 and 30% of newly synthesized proteins are degraded by the UPS as a result of misfolding or translational errors, and that proteasome targets are mostly newly-synthesized[52,65]. Since HS increases the rate of protein misfolding, we were interested to see what proportion of the ubiquitinated proteins after HS are newly translated. Using a pulse SILAC combined with diGly enrichment method, we identified a subset of ubiquitinated proteins that are newly synthesized upon HS. Surprisingly however, 60% of the ubiquitinated proteins also quantified in the TCL correspond to pre-existing proteins indicating that HS leads to the ubiquitination of mostly pre-existing proteins. Upon GO analysis of this group, proteins involved in DNA metabolic processes, such as RNA polymerase II and DNA mismatch repair protein Msh6, were most significantly enriched

(Table A4). This indicates that ubiquitination may play an important role the universal repression of transcription that occurs upon HS.

Our experiments still revealed that a large portion of newly-synthesized proteins are also getting ubiquitinated under stress. This group comprised of 40% of the total proteins that were also quantified in the TCL. This was expected as these proteins not being properly folded at the time of stress could cause them to fold improperly and thus be ubiquitinated. Amongst this group of newly-synthesized proteins, there was a small but significant enrichment for the CCT (chaperonin containing TCP-1) complex, and more significant enrichment for components of the ribosome and the Nop56p-associated pre-rRNA complex, which is required for the assembly of the 60S ribosomal subunit. CCT is chaperone that is usually involved in proper protein folding[66]. Its HS-dependent ubiquitination upon synthesis of only a specific subgroup of proteins is therefore puzzling. It could be that cells prevent the increase the folding capacity of that group of chaperones to favour instead the accumulation of vital HSPs during the HS response. Additionally, it has been recently found that UBE2O, an E2 conjugating enzyme, can independently ubiquitinate newly made orphan proteins that arise under proteotoxic stress[67]. More specifically, it ubiquitinates ribosomal components RPL8, RPL24, and RPL3, of which the latter was found in our pulse SILAC experiment, which prevents their nuclear import and targets them for degradation. The enrichment of ubiquitinated newly-synthesized/orphan ribosomal components upon HS that we observed could therefore be a result of orphan protein PQC involving UBE2O and other UPS members. Alternatively, the proteins that we identified that are involved in ribosome biogenesis could be sequestered in the nucleus by their ubiquitination upon HS and thus impeding translation as is has been previously shown in yeast[68]. Further studies are needed to show the sub-cellular

location of these ubiquitinated newly-synthesized proteins upon HS to gain a better understanding of the processes involved.

4.2. The Role of Nedd4-1 and Itch in the Hek293 HS Ubiquitination Response.

As our GlyGly experiments were done in Hek293 cells, we wanted to determine which E3 ligase was responsible for the increase in ubiquitination after HS. Despite previous studies that identified Nedd4-1 as the main E3 ligase responsible for an increase in ubiquitination levels upon HS in MEF and HeLa cells, we did not observe a similar result in Hek293 cells. When we looked at more specific changes in the ubiquitination patterns, we saw that there was a decrease in both soluble and insoluble ubiquitin conjugates when Nedd4-1 was knocked down. This could indicate that Nedd4-1 could play a minor role in ubiquitinating soluble proteins. Nonetheless, Nedd4-1 is not the main E3 ligase responsible for the HS ubiquitination response in Hek293 cells.

Instead, we found that among all Nedd4 family members, cells expressing shRNA that targets Itch displayed the most drastic impairment of the HS ubiquitination response. We were able to confirm these results using four shRNA targeting four different regions of Itch mRNA. Therefore, it is unlikely that off target effects could explain the results. However, we were unable to restore HS-dependent ubiquitination levels when Itch was added back to KD cells, as well as control cells, despite its overexpression. The excess amount of Itch could potentially have had inhibitory effects. It could be due to an accumulation of Itch in the endoplasmic reticulum (ER), exceeding the folding capacity of the ER, or could just cause some sort of dominant negative effect on the cell by outcompeting other factors required for the response. The study of Itch has mainly been done in relation to inflammation. It has been shown to regulate the immune system: mutant mice develop a severe inflammatory disease and develop

autoimmunity, and ITCH deficient humans develop an autoimmune disease[69,70]. Itch notably targets p73, a transcription factor that promotes the expression of pro-apoptotic genes, for proteasomal degradation, implicating it in the regulation of chemotherapeutic agent-induced apoptotic cell death[71,72]. Interestingly, it has also been shown to target cytosolic misfolded proteins during proteotoxic cell death caused by polyglutamine huntingtin proteins[73]. Since Itch has shown to play a role in various stress responses, its involvement in the HS response is maybe not surprising.

When investigating the effect that Itch had on Hek293 cell viability, we observed that the lack of Itch caused a noticeable drop in the percentage of cells alive after severe HS at an earlier timepoint as compared to control cells. In other words, the KD cells were unable to cope with the stress as long as the control cells, and underwent death at a sooner time point. Heat stress is known to induce apoptosis and necrosis upon HS, and the portion of cells undergoing either one varies depending on the severity of the HS[74]. As previously mentioned, Itch is involved in the negative regulation of apoptosis[71]. Therefore, the absence of Itch could cause certain proteins in apoptosis to no longer be repressed leading to a faster rate of cell death. As it is unknown what proportion of Itch-dependent cell death is apoptosis or necrosis, the same could be said for proteins involved in necrosis. Further investigation of the type of cell death occurring upon HS could help to decipher between these two possibilities.

4.3. Confirming the Role of Nedd4-1 in the MEF HS Ubiquitination Response.

Although we did not identify Nedd4-1 as the main E3 ligase responsible for the increase in ubiquitination in Hek293 cells, we did confirm that it is in MEF cells. We also

showed that both K48 and K63-linked polyubiquitination increased after HS in a Nedd4-1 dependent manner. Although Nedd4-1 mainly conjugates K63 chains, the increase in K48 chains could be attributed to Nedd4-1 targeting misfolded proteins that occur due to the heat stress to the proteasome for degradation. There is also an increase in K63 chains, indicating that Nedd4-1 could potentially be also targeting misfolded proteins for lysosomal degradation. Nedd4-1 has previously been shown to positively regulate autophagy by ubiquitinating LC3, and this regulation could increase upon HS[75].

Due to the conflicting data between the Hek293 Nedd4-1 knockdown and MEF Nedd4-1 -/- cells, we wanted to add-back Nedd4-1 into the MEF Nedd4 -/- cells and see if it would restore the increased ubiquitination upon HS as well as cell viability. By doing this, we would be able to determine if the effect that we observed with the -/- cells can be attributed to Nedd4-1 being knocked out or due to an off-target effect. After multiple attempts, we were unsuccessful at transfecting Nedd4-1 into the cells and it was thereafter confirmed to us that these cells are difficult to transfect (personal communication from Dr. Rotin). Finally, we determined that Nedd4-1 in MEF cells was crucial for its viability under duress. As with Itch in Hek293 cells, it could be responsible for either the degradation of pro-apoptotic or pro-necroptotic proteins or both, and its absence reflects the cell's inability to cope with heat-stress as well as WT cells.

Why are two different Nedd4 E3 ligase family members required in different cell types? While we showed that KD of Nedd4-1 largely impairs the increased ubiquitination upon HS in HeLa cells[28], it did not in Hek293 cells. The role that Itch plays in this response in HeLa cells unknown. Nevertheless, our results clearly show that different E3s are required in different cell types. Nedd4-1 is similarly expressed in both Hek293 and HeLa cells[76], however

Nedd4-1 is the most highly expressed family member in mouse embryonic tissue (over 5 times more than Itch)[77]. Its abundance could be reflective of its importance in MEF cells and thus its implication in their HS ubiquitination response is not surprising. Itch is highly expressed in Hek293 and HeLa cells and at similar levels to Nedd4-1 and Nedd4L, whereas all other Nedd4 family members are expressed at much lower levels[76]. Although these E3 ligases have similar abundance levels when unstressed, Nedd4-1 numbers could rapidly increase in HeLa cells upon HS and not in Hek293 cells. In addition, in MEFs, Nedd4-1 is cytosolic under normal conditions, whereas upon HS, it partially relocalizes to the nucleus[78]. The difference between cell lines in reference to the involvement of this E3 in the HS response could be due to localization, where it could relocalize in some cell lines and not in others. Furthermore, different substrate adaptors may play a role in the mammalian HS ubiquitination response as we have seen in yeast with Ydj1, an Hsp40 chaperone[28]. It could be that different Hsp40 proteins are differentially expressed in different cell types and may have different affinities for different Nedd4 family members. Finally, Nedd4 family E3 ligases are all auto-inhibited and require different mechanisms/proteins to release this inhibition and activate them[79]. It could be possible that the rate of release from auto-inhibition of Nedd4-1 differs between cell lines upon HS, dependent on the availability or expression of components involved in their inhibition relief.

Chapter 5 - Conclusion

Understanding the HS response in mammalian cells is crucial for developing therapeutic targets to combat diseases that may arise from misfolded proteins that trigger this response. It is also critical to know how extreme heat affects the cell as HS is often used alone or in combination with radiation or chemotherapy to treat different forms of cancer[80]. There has been extensive characterization of the HS response in terms of the action of stress-induced HS proteins and other HS factors such as HSF1, however realistically all cell compartments and biological processes are affected by HS to some degree[9,81–83]. Given the important role that the UPS plays in cellular proteostasis, it is surprising that more work has not been done to describe its role in the HS response and uncover key players which could be potential drug targets.

In this study, we acquired a list of proteins that are ubiquitinated upon HS and gained some insight into the crossover between the UPS and other cellular processes, as well as some common features of these proteins. Although we garnered some useful information from this set of experiments, our coverage of the HS ubiquitinome was lower than what is possible. To gain more confidence in our results and uncover more proteins, it would be useful to employ certain techniques, such as GlyGly bead cross-linking and fractionation prior to MS analysis, which has been done to improve identification to thousands of sites[84].

We now know that some processes are significantly ubiquitinated upon HS, such as pre-mRNA processing and SUMOylation, however we do not know the fate of the proteins involved in them. It is unclear whether they are being targeted for degradation through the proteasome or autophagy or both, or if they are simply being targeted to an area of the cell

where they are sequestered until the stress is gone. One future direction would be to pick some candidates from our list that are heavily involved in one of these processes and track their localization and rate of degradation by fluorescent tags or radioactive pulse chase assays[85]. These experiments would also help us better understand the fate of ubiquitinated newly-synthesized ribosome components upon HS. It is unclear if any of them can enter the nucleus during stress. Screening for their protein-protein interactions could also potentially uncover other E3 ligases are involved in orphan protein PQC.

With initial expectations that Nedd4-1 is mainly responsible for these identified GlyGly sites in Hek293 cells, it was surprising that Itch instead seems to play the bigger role in the HS ubiquitination response. Because of our conflicting results between different cells lines, it would be interesting to evaluate the role of these two E3s, as well as Nedd4L (due to abundance), in a wide variety of cell lines to see if we can observe a trend, or if one is more universally predominant than the other. We could firstly evaluate the effect that an Itch KD has in HeLa cells. It would be intriguing to look at neuronal cells as well because of the interaction of Nedd4-1 with α-synuclein and Lewy bodies[4]. The role of Itch in the HS response in Hek293 cells also needs to be re-evaluated, by doing MS and western blot analysis in parallel, as well as GlyGly enrichment protocol optimization.

Finally, although our MS data did not validate our Itch KD western blot results, the lack of Itch negatively effected the viability of Hek293 cells under severe HS. We also showed that the correlation between decreased ubiquitination and decreased viability exists in MEF Nedd4 -/- cells. A future experiment could look at the behaviour necrosis and apoptosis factors during HS. This has been done previously where post-HS analysis by flow cytometry was used to measure the incidences of apoptosis (annexin V-FITC stain), necrosis (propidium

iodide stain), and HSP70 transcription (GFP-tagged)[74]. Such analysis could be used to observe the role that Itch/Nedd4-1 have on the presence or absence of these factors.

Bibliography

1. Pilla, E., Schneider, K. & Bertolotti, A. Coping with Protein Quality Control Failure. *Annu. Rev. Cell Dev. Biol.* **33,** (2017).

2. Baets, G. De, Doorn, L. Van, Rousseau, F. & Schymkowitz, J. Increased Aggregation Is More Frequently Associated to Human Disease-Associated Mutations Than to Neutral Polymorphisms. *PLOS Comput. Biol.* 1–14 (2015). doi:10.1371/journal.pcbi.1004374

3. Schymkowitz, J. & Rousseau, F. A rescue by chaperones. *Nat. Chem. Biol.* 1–4 (2016). doi:10.1038/nchembio.2006

4. Schulz-Schaeffer, W. J. The synaptic pathology of a -synuclein aggregation in dementia with Lewy bodies , Parkinson ' s disease and Parkinson ' s disease dementia. *Acta Neuropathol.* **120,** 131–143 (2010).

5. Richter, K., Haslbeck, M. & Buchner, J. Review The Heat Shock Response : Life on the Verge of Death. *Mol. Cell* **40,** 253–266 (2010).

6. Mahat, D. B., Salamanca, H. H., Duarte, F. M., Danko, C. G. & Lis, J. T. Mammalian Heat Shock Response and Mechanisms Underlying Its Genome-wide Transcriptional Regulation. *Mol. Cell* **62,** 63–78 (2016).

7. Spriggs, K. A., Bushell, M. & Willis, A. E. Translational Regulation of Gene Expression during Conditions of Cell Stress. *Mol. Cell* **40,** 228–237 (2010).

8. Shalgi, R., Hurt, J. A., Lindquist, S. & Burge, C. B. Widespread inhibition of posttranscriptional splicing shapes the cellular transcriptome following heat shock. *Cell Rep.* **7,** 1362–1370 (2014).

9. Velichko, A., Markova, E., Petrova, N., Razin, S. & Kantidze, O. Mechanisms of heat shock response in mammals. *Cell. Mol. Life Sci.* (2014). doi:10.1007/s00018-013-1348-7

10. Hartl, F. U., Bracher, A. & Hayer-Hartl, M. Molecular chaperones in protein folding and proteostasis. *Nature* **475,** 324–332 (2011).

11. Park, C. & Cuervo, A. Selective Autophagy : talking with the UPS. *Cell Biochem Biophys* **67,** 3–13 (2013).

12. Korolchuk, V. I. *et al.* A novel link between autophagy and the ubiquitin-proteasome system. *Autophagy* **5,** 862–863 (2009).

13. Kwon, Y. T. & Ciechanover, A. The Ubiquitin Code in the Ubiquitin-Proteasome System and Autophagy. *Trends Biochem. Sci.* **42,** 873–886 (2017).

14. Medicherla, B. & Goldberg, A. L. Heat shock and oxygen radicals stimulate ubiquitin-dependent degradation mainly of newly synthesized proteins. *J. Cell Biol.* **182,** 663–673 (2008).

15. Komander, D. & Rape, M. The Ubiquitin Code. *Annu. Rev. Biochem.* **81,** 203–229 (2012).

16. Hershko, a & Ciechanover, a. The ubiquitin system. *Annu. Rev. Biochem.* **67,** 425–479 (1998).

17. Yau, R. & Rape, M. The increasing complexity of the ubiquitin code. *Nat. Cell Biol.* **18,** 579–586 (2016).

18. Kaliszewski, P. & Zoładek, T. The role of Rsp5 ubiquitin ligase in regulation of diverse processes in yeast cells. *Acta Biochim. Pol.* **55,** 649–662 (2008).

19. Hershko, Avram; Ciechanover, A. The Ubiquitin System. *Annu. Rev. Biochem.* **67,** 425–479 (1998).

20. Berndsen, C. & Wolberger, C. New insights into ubiquitin E3 ligase mechanism. *Nat. Struct. Mol. Biol.* **21,** 301–307 (2014).

21. Rotin, D. & Kumar, S. Physiological functions of the HECT family of ubiquitin ligases. *Nat. Rev. Mol. Cell Biol.* **10,** 398–409 (2009).

22. Wilkinson, K. D. Ubiquitination and deubiquitination: targeting of proteins for degradation by the proteasome. *Cell Dev. Biol.* **11,** 141–148 (2000).

23. Rajalingam, K. & Dikic, I. SnapShot: Expanding the Ubiquitin Code. *Cell* **164,** 1074–1074.e1 (2016).

24. Glickman, M. H. & Ciechanover, A. The Ubiquitin-Proteasome Proteolytic Pathway : Destruction for the Sake of Construction. 373–428 (2002).

25. Tanaka, K. The proteasome: Overview of structure and functions. *Proc. Jpn. Acad., Ser. B* **85,** (2009).

26. Johnson, D. E. The ubiquitin – proteasome system: opportunities for therapeutic intervention in solid tumors. *Endocr. Relat. Cancer* **22,** 1–17 (2015).

27. Parag, H. A., Raboy, B. & Kulka, R. G. Effect of heat shock on protein degradation in mammalian cells: involvement of the ubiquitin system. *EMBO* **6,** 55–61 (1987).

28. Fang, N. N. *et al.* Rsp5/Nedd4 is the main ubiquitin ligase that targets cytosolic misfolded proteins following heat stress. *Nat. Cell Biol.* **16,** 1227–1237 (2014).

29. Fang, N. N., Zhu, M., Rose, A., Wu, K. & Mayor, T. Deubiquitinase activity is required for the proteasomal degradation of misfolded cytosolic proteins upon heat-stress. *Nat. Commun.* **7,** 1–16 (2016).

30. Ingham, R. J., Gish, G. & Pawson, T. The Nedd4 family of E3 ubiquitin ligases: functional diversity within a common modular architecture. *Oncogene* **23,** 1972–1984 (2004).

31. Boase, N. A. & Kumar, S. NEDD4 : The founding member of a family of ubiquitin-protein ligases. *Gene* **557,** 113–122 (2015).

32. Bruce, M. C. *et al.* Regulation of Nedd4-2 self-ubiquitination and stability by a PY motif located within its HECT-domain. *Biochem. J.* **415,** 155–163 (2008).

33. Zhu, K. *et al.* Allosteric auto-inhibition and activation of the Nedd4 family E3 ligase Itch. *EMBO Rep.* **18,** e201744454 (2017).

34. Chen, Z. *et al.* A Tunable Brake for HECT Ubiquitin Ligases. *Mol. Cell* **66,** 345–357.e6 (2017).

35. Shearwin-Whyatt, L., Dalton, H. E., Foot, N. & Kumar, S. Regulation of functional diversity within the Nedd4 family by accessory and adaptor proteins. *BioEssays* **28,** 617–628 (2006).

36. Snyder, P. M., Steines, J. C. & Olson, D. R. Relative Contribution of Nedd4 and Nedd4-2 to ENaC Regulation in Epithelia Determined by RNA Interference. *J. Biol. Chem.* **279,** 5042–5046 (2004).

37. Noyes, N. C., Hampton, B., Migliorini, M. & Strickland, D. K. Regulation of Itch and Nedd4 E3 Ligase Activity and Degradation by LRAD3. *Biochemistry* **55,** 1204–1213 (2016).

38. Kelly, S. M., Vanslyke, J. K. & Musil, L. S. Regulation of Ubiquitin-Proteasome System – mediated Degradation by Cytosolic Stress. *Mol. Biol. Cell* **18,** 4279–4291 (2007).

39. Golebiowski, F. *et al.* System-Wide Changes to SUMO Modifications in Response to Heat Shock. **2,** (2009).

40. Tammsalu, T. *et al.* Proteome-wide Identification of SUMO2 Modification Sites. *Sci Signal* **7,** (2014).

41. Yaoyang Zhang, Bryan R. Fonslow, Bing Shan, Moon-Chang Baek, and J. R. & Yates. Protein Analysis by Shotgun/Bottom-up Proteomics. *Chem. Rev.* **113,** 2343–2394 (2013).

42. Peng, J. *et al.* A proteomics approach to understanding protein ubiquitination. *Nat. Biotechnol.* **21,** 921–926 (2003).

43. Lichti, C. et al. in *Genomics and Proteomics for Clinical Discovery and Development* (2014).

44. Xu, G., Paige, J. S. & Jaffrey, S. R. Global analysis of lysine ubiquitination by ubiquitin remnant immunoaffinity profiling. *Nat. Biotechnol.* **28,** 868–873 (2011).

45. Kim, W. *et al.* Systematic and Quantitative Assessment of the Ubiquitin-Modified Proteome. *Mol. Cell* **44,** 325–340 (2011).

46. Wagner, S. A. *et al.* Proteomic Analyses Reveal Divergent Ubiquitylation Site Patterns in Murine Tissues. *Mol. Cell. Proteomics* **11,** 1578–1585 (2012).

47. Wagner, S. A. *et al.* A Proteome-wide, Quantitative Survey of In Vivo Ubiquitylation Sites Reveals Widespread Regulatory Roles. *Mol. Cell. Proteomics* **10,** M111.013284 (2011).

48. Fouladkou, F. *et al.* The ubiquitin ligase Nedd4-1 is dispensable for the regulation of PTEN stability and localization. *PNAS* **105,** 8585–8590 (2008).

49. Rappsilber, J., Mann, M. & Ishihama, Y. Protocol for micro-purification, enrichment, pre-fractionation and storage of peptides for proteomics using StageTips. *Nat. Protoc.* **2,** 1896–1906 (2007).

50. Beck, S. *et al.* The Impact II, a Very High-Resolution Quadrupole Time-of-Flight Instrument (QTOF) for Deep Shotgun Proteomics. *Mol. Cell. Proteomics* **14,** 2014–2029 (2015).

51. Dammer, E. B. *et al.* Polyubiquitin linkage profiles in three models of proteolytic stress suggest the etiology of alzheimer disease. *J. Biol. Chem.* **286,** 10457–10465 (2011).

52. Kim, W. *et al.* Systematic and quantitative assessment of the ubiquitin modified proteome. *Mol. Cell* **44,** 325–340 (2011).

53. Kim, H. C. & Huibregtse, J. M. Polyubiquitination by HECT E3s and the Determinants of Chain. *Mol. Cell. Biol.* **29,** 3307–3318 (2009).

54. Hjerpe, R. *et al.* UBQLN2 Mediates Autophagy-Independent Protein Aggregate Clearance by the Proteasome. *Cell* **166,** 935–949 (2016).

55. Fang, N., Ng, A., Measday, V. & Mayor, T. Hul5 HECT Ubiquitin Ligase Plays A Major Role in The Ubiquitylation and Turn Over of Cytosolic Misfolded Proteins. *Nat. Cell Biol.* **13,** 1344–1352 (2011).

56. Gatti, M. *et al.* RNF168 promotes noncanonical K27ubiquitination to signal DNA damage. *Cell Rep.* **10,** 226–238 (2015).

57. Velichko, A. K., Petrova, N. V., Kantidze, O. L. & Razin, S. V. Dual effect of heat shock on DNA replication and genome integrity. *Mol. Biol. Cell* **23,** 3450–3460 (2012).

58. Turner, T. & Caspari, T. When heat casts a spell on the DNA damage checkpoints. *Open Biol.* **4,** 140008–140008 (2014).

59. Nakata, S. *et al.* The dynamics of histone H2A ubiquitination in HeLa cells exposed to rapamycin, ethanol, hydroxyurea, ER stress, heat shock and DNA damage. *Biochem. Biophys. Res. Commun.* **472,** 46–52 (2016).

60. Yau, R. G. *et al.* Assembly and Function of Heterotypic Ubiquitin Chains in Cell-Cycle and Protein Quality Control. *Cell* **171,** 918–933.e20 (2017).

61. Labbadia, J. *et al.* Mitochondrial Stress Restores the Heat Shock Response and Prevents Proteostasis Collapse during Aging. *Cell Rep.* **21,** 1481–1494 (2017).

62. Matic, I. *et al.* Proteome-wide identification of SUMO modification sites by mass spectrometry. *Nat. Protoc.* **10,** 1374–1388 (2015).

63. Alteri, C. J., Lindner, J. R., Reiss, D. J., Smith, S. N. & Harry, L. T. RNF4-Dependent Hybrid SUMO-Ubiquitin Chains are Signals for RAP80 and thereby Mediate the Recruitment of BRCA1 to Sites of DNA Damage. *Signalling* **82,** 145–163 (2012).

64. Hendriks, I. A. *et al.* Site-specific mapping of the human SUMO proteome reveals co-modification with phosphorylation. *Nat. Struct. Mol. Biol.* **24,** 325–336 (2017).

65. Yewdell, J. W. & Nicchitta, C. V. The DRiP hypothesis decennial: support, controversy, refinement and extension. *Trends Immunol.* **27,** 368–373 (2006).

66. Pavel, M. *et al.* CCT complex restricts neuropathogenic protein aggregation via autophagy. *Nat. Commun.* **7,** (2016).

67. Yanagitani, K. & Juszkiewicz, S. UBE2O is a quality control factor for orphans of multiprotein complexes. **475,** 472–475 (2017).

68. Cherkasov, V. *et al.* Systemic control of protein synthesis through sequestration of translation and ribosome biogenesis factors during severe heat stress. *FEBS Lett.* **589,** 3654–3664 (2015).

69. Aki, D., Zhang, W. & Liu, Y. C. The E3 ligase Itch in immune regulation and beyond. *Immunol. Rev.* **266,** 6–26 (2015).

70. Lohr, N. J. *et al.* Human ITCH E3 Ubiquitin Ligase Deficiency Causes Syndromic Multisystem Autoimmune Disease. *Am. J. Hum. Genet.* **86,** 447–453 (2010).

71. Rossi, M. *et al.* The ubiquitin-protein ligase Itch regulates p73 stability. *EMBO J.* **24,** 836–848 (2005).

72. Hansen, T. M. *et al.* Itch inhibition regulates chemosensitivity in vitro. *Biochem. Biophys. Res. Commun.* **361,** 33–36 (2007).

73. Chhangani, D., Upadhyay, A., Amanullah, A., Joshi, V. & Mishra, A. Ubiquitin ligase ITCH recruitment suppresses the aggregation and cellular toxicity of cytoplasmic misfolded proteins. *Sci. Rep.* **4,** 1–12 (2014).

74. Song, A. S., Najjar, A. M. & Diller, K. R. Thermally Induced Apoptosis, Necrosis, and Heat Shock Protein Expression in 3D Culture. *J. Biomech. Eng.* **136,** 71006 (2014).

75. Sun, A. *et al.* The E3 ubiquitin ligase NEDD4 is an LC3-interactive protein and regulates autophagy. *Autophagy* **13,** 522–537 (2017).

76. Geiger, T., Wehner, A., Schaab, C., Cox, J. & Mann, M. Comparative Proteomic Analysis of Eleven Common Cell Lines Reveals Ubiquitous but Varying Expression of Most Proteins. *Mol. Cell. Proteomics* **11,** M111.014050 (2012).

77. Geiger, T. *et al.* Initial Quantitative Proteomic Map of 28 Mouse Tissues Using the SILAC Mouse. *Mol. Cell. Proteomics* **12,** 1709–1722 (2013).

78. Zhao, Z., Dammert, M. A., Hoppe, S., Bierhoff, H. & Grummt, I. Heat shock represses rRNA synthesis by inactivation of TIF-IA and lncRNA-dependent changes in nucleosome positioning. *Nucleic Acids Res.* **44,** 8144–8152 (2016).

79. Fajner, V., Maspero, E. & Polo, S. Targeting HECT-type E3 ligases – insights from catalysis, regulation and inhibitors. *FEBS Lett.* **591,** 2636–2647 (2017).

80. Peeken, J. C., Vaupel, P., Combs, S. E. & Combs, S. E. Integrating Hyperthermia into Modern Radiation Oncology: What Evidence Is Necessary? *Front. Oncol.* **7,** (2017).

81. Colaco, C. A., Bailey, C. R., Walker, K. B. & Keeble, J. Heat Shock Proteins : Stimulators of Innate and Acquired Immunity. *Biomed Res. Int.* **2013,** (2013).

82. Bakthisaran, R., Tangirala, R. & Rao, C. M. Small heat shock proteins : Role in cellular functions and pathology. *BBA - Proteins Proteomics* **1854,** 291–319 (2015).

83. Li, J., Labbadia, J. & Morimoto, R. I. Rethinking HSF1 in Stress , Development , and Organismal Health. *Trends Cell Biol.* **27,** 895–905 (2017).

84. Udeshi, N. D., Mertins, P., Svinkina, T. & Carr, S. A. Large-Scale Identification of Ubiquitination Sites by Mass Spectrometry. *Nat. Methods* **8,** 1950–1960 (2013).

85. Mossuto, M. F. *et al.* A Dynamic Study of Protein Secretion and Aggregation in the Secretory Pathway. *PLoS One* **9,** (2014).

Appendix

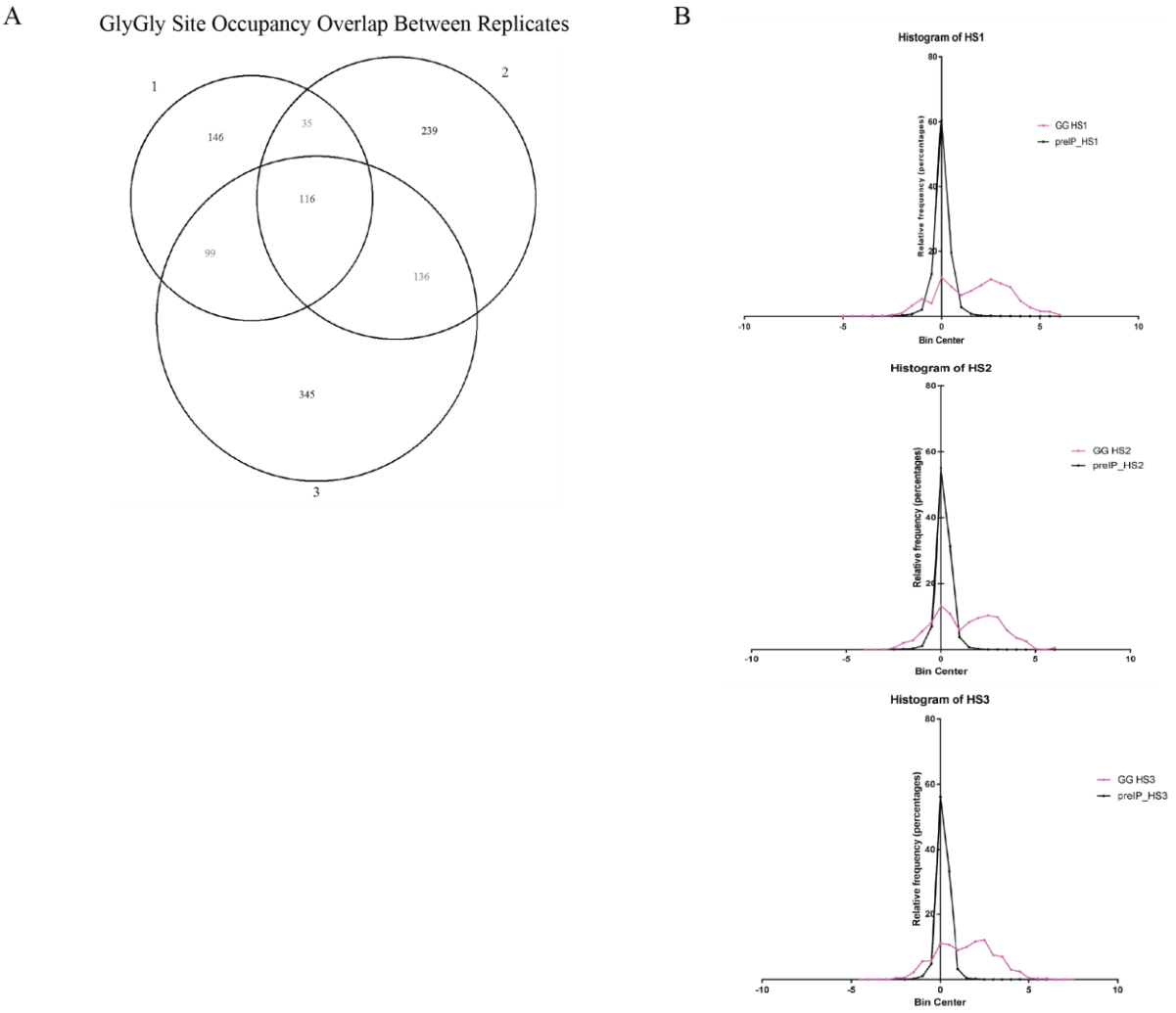

Figure A.1. GlyGly Site Occupancy of HS SILAC Replicates.

(A) Comparison of quantified HS-dependent GlyGly site IDs between 3 replicates. **(B)** Frequency distributions (%) of each replicate, comparing their $\log_2$(L/H) ratio distribution to their TCL counterparts. Graph was created using Perseus. The cut-off for GlyGly sites enriched after HS was determined by 2 standard deviations from mean (95% CI). Cut-offs were 0.95214, 0.9865, and 0.997 for replicates 1, 2, and 3 respectively.

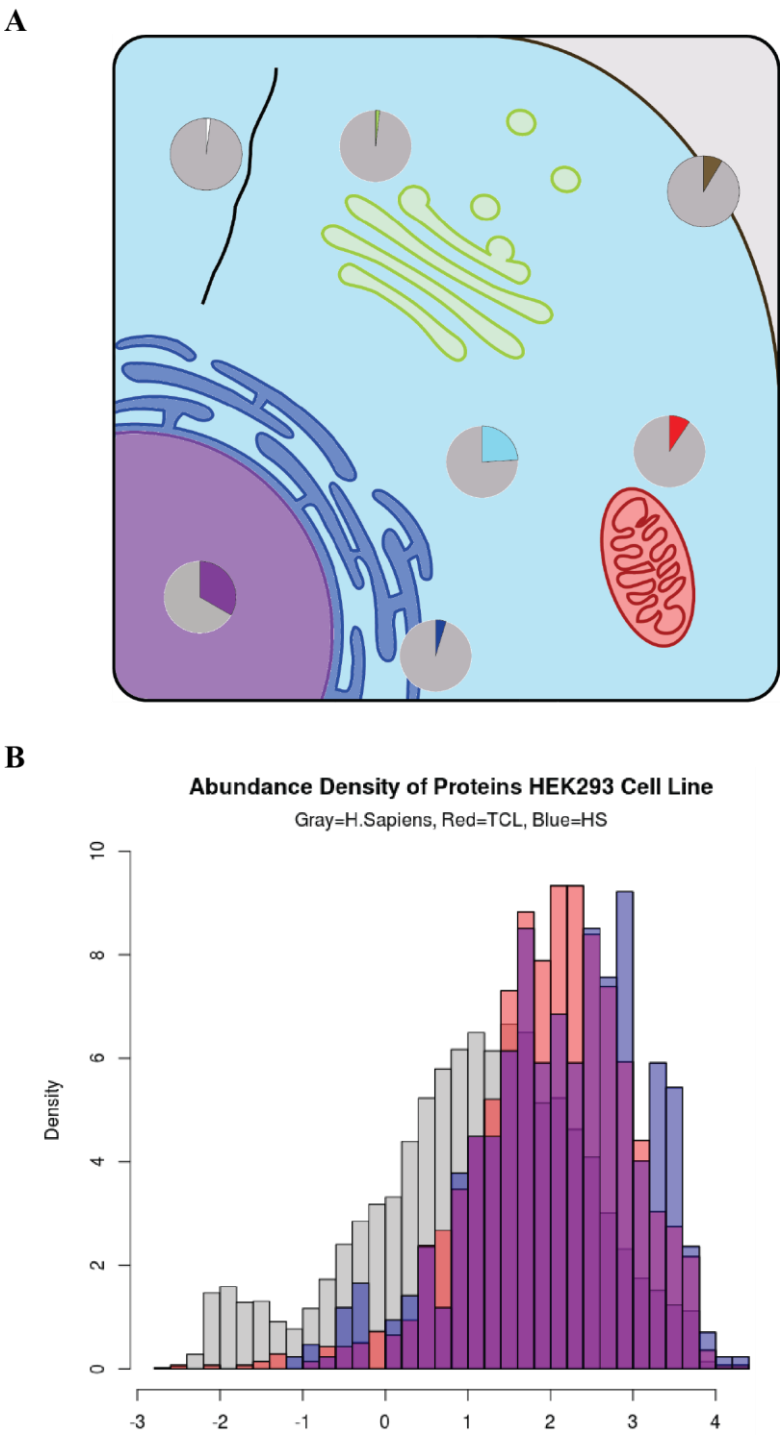

Figure A.2. Localization and Abundance of TCL Proteins from HS SILAC Replicates.

(A) Subcellular localization of the proteins associated with the quantified peptides from TCL samples (nucleus = purple, ER = dark blue, cytosol = blue, mitochondria = red, cytoskeleton = white, Golgi = green, plasma membrane = brown). Pie-chart is the proportion of proteins primarily associated with that compartment out of the 1761 proteins identified (also summarized in Table A.1.). **(B)** Comparison of the abundance density in all 3 GlyGly (blue) and TCL (red) replicates to the Hek293 proteome (grey). Data was obtained from https://pax-db.org/.

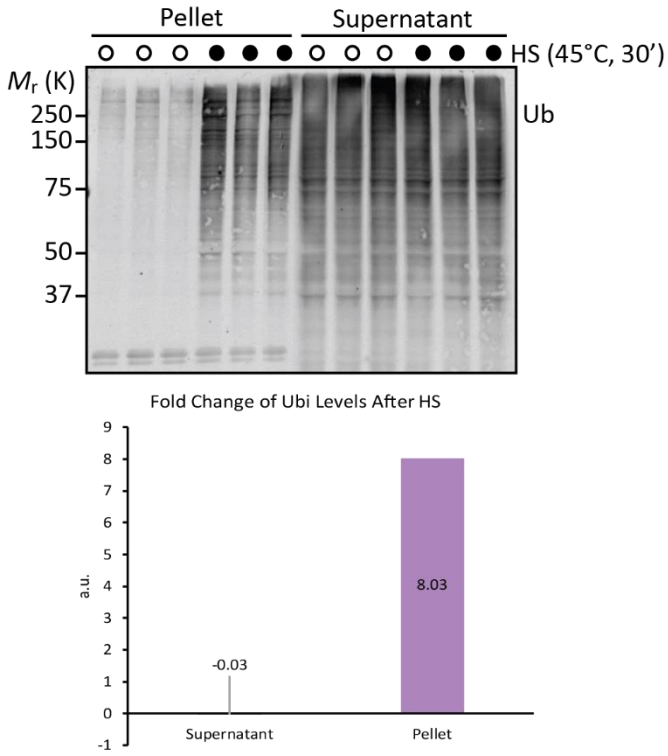

Figure A.3. Ubiquitination Levels of Soluble and Insoluble Fractions of MEF Cells Upon HS.

Ubiquitination levels of MEF WT cells before and after HS following the separation of each sample into pellet and supernatant fractions (3 biological replicates for each condition). Levels were averaged between replicates for each condition prior to calculating fold change (shown in graph below).

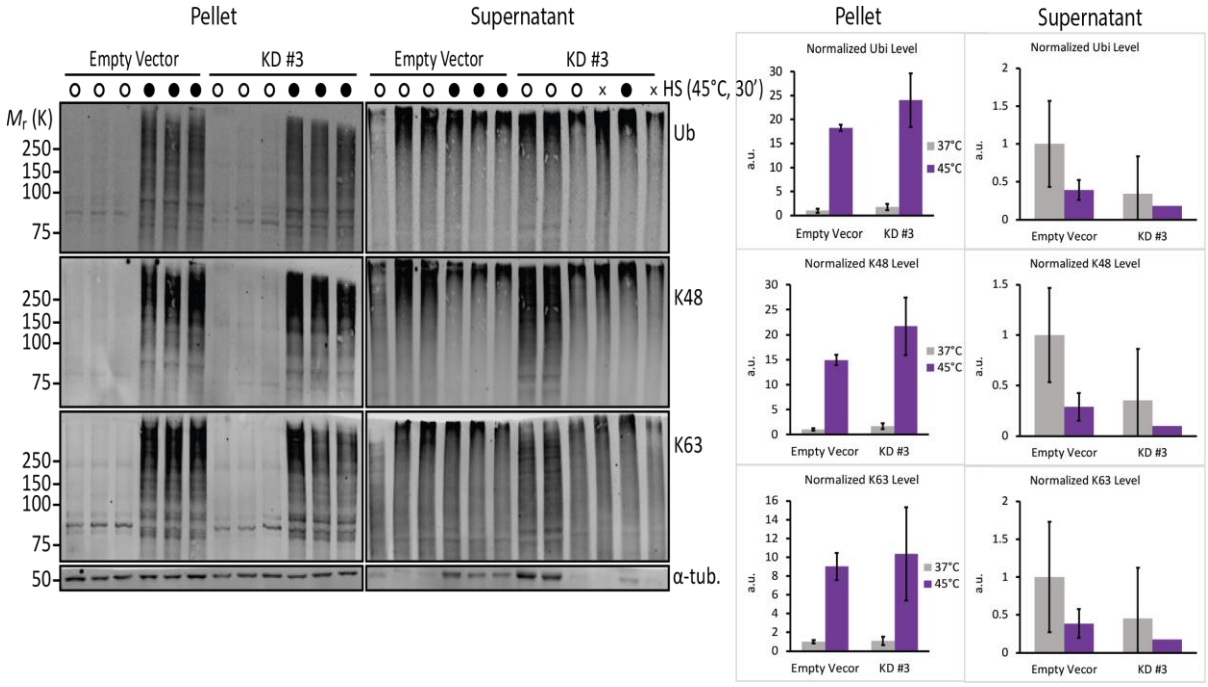

Figure A.4. Nedd4-1 KD Effects on Ubiquitination of Soluble and Insoluble Conjugates is Inconsistent.

Total, K48-, and K63-ubiquitination levels of empty vector control cells and Nedd4-1 KD #3 cells before (open circle) and after HS (black) following the separation of each sample into pellet and supernatant fractions (3 biological replicates for each condition; with the exception of a couple samples that were mishandled marked by an "x"). Beside the blots is the quantification of ubiquitin levels normalized to α-tubulin.

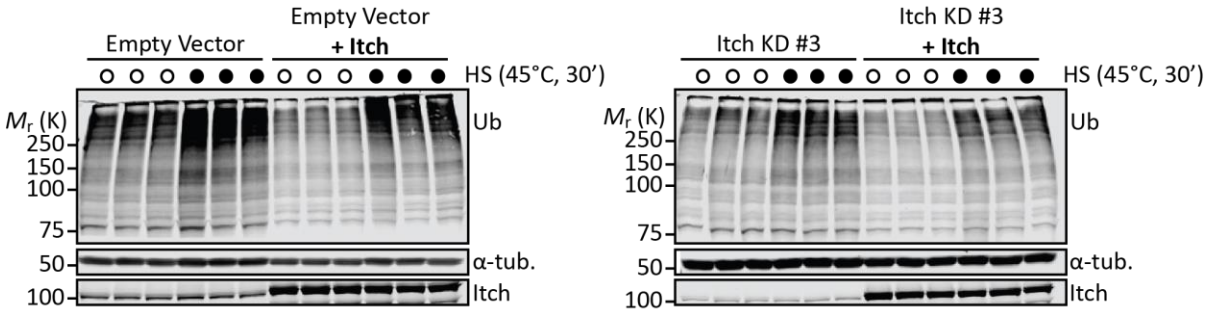

Figure A.5. Itch Addback Ubiquitination Levels in Itch KD Cells After HS.

Ubiquitination levels in Itch KD #3 cells (right) or empty vector control cells (left) compared to the same cells where Itch was added back and overexpressed before (open circle) and after HS (black). Analysed by western blots and normalized to α-tubulin (3 biological replicated for each condition).

Table A.1. Localization of Ubiquitinated Proteins Upon HS Compared to TCL.

Cell Compartment	GlyGly (%)	TCL (%)
Nucleus	60	33
Cytosol	43	24
Mitochondria	3	9
Cytoskeleton	2	2
Plasma Membrane	5	5
Endoplasmic Reticulum	3	5
Golgi	2	2

Table A.2. GO Analysis of Ubiquitinated Proteins Enriched Upon HS.

GO Annotation	GO Term	No. in Category	p-value
GO:0016071	mRNA Metabolic Process	71	6.72E-30
REAC:72203	Processing of Capped Intron-Containing Pre-mRNA	32	4.55E-14
KEGG:03013	RNA Transport	18	3.71E-06
REAC:2990846	SUMOylation	16	7.06E-06
KEGG:03040	Spliceosome	15	2.57E-05
REAC:69278	Cell Cycle, Mitotic	32	3.07E-05
REAC:73894	DNA Repair	23	9.40E-05
REAC:72649	Translation Initiation Complex Formation	10	1.61E-04

Table A.3. GO Analysis of Newly-Synthesized Ubiquitinated Proteins Enriched Upon HS.

GO Annotation	GO Term	No. in Category	p-value
CORUM:306	Ribosome	17	6.43E-16
CORUM:3055	Nop56p-associated pre-rRNA complex	14	1.06E-09
CORUM:126	CCT complex (chaperonin containing TCP1 complex)	3	3.00E-02

Table A4. GO Analysis of Pre-Existing Ubiquitinated Proteins Enriched Upon HS.

GO Annotation	GO Term	No. in Category	p-value
GO:0006259	DNA Metabolic Process	23	3.83E-12
GO:0051129	Negative Regulation of Cellular Component Organization	11	3.64E-03
GO:0006278	RNA-Dependent DNA Biosynthetic Process	5	4.12E-03
GO:2001242	Regulation of Intrinsic Apoptotic Signaling Pathway	6	1.64E-02
GO:0000413	Protein Peptidyl-Prolyl Isomerization	4	1.92E-02
GO:0006606	Protein Import into Nucleus	7	3.41E-02

Table A.5. List of shRNA Used to Generate Hek293 KD Stable Cell Lines in this Study.

Stable Cell Line	shRNA TRC #	Sequence	Target Region
Nedd4-1 KD #1	TRCN0000007550	CCGGGCCTTTCTCTTGCCTGCAT ATCTCGAGATATGCAGGCAAGA GAAAGGCTTTTT	3UTR
Nedd4-1 KD #2	TRCN0000007551	CCGGCCGGAGAATTATGGGTGT CAACTCGAGTTGACACCCATAA TTCTCCGGTTTTT	CDS
Nedd4-1 KD #3	TRCN0000007553	CCGGGCTGAACTATACGGTTCA AATCTCGAGATTTGAACCGTAT AGTTCAGCTTTTT	CDS
Nedd4-1 KD #4	TRCN0000007554	CCGGCGGTTGGAGAATGTAGCA ATACTCGAGTATTGCTACATTCT CCAACCGTTTTT	CDS
Nedd4L KD #1	TRCN0000000904	CCGGCCTGTTTGTATGCGTTTGCT ACTCGAGTAGCAAACGCATACA AACAGGTTTTT	3UTR
Nedd4L KD #2	TRCN0000000905	CCGGCGCCTTGACTTACCTCCA TATCTCGAGATATGGAGGTAAG TCAAGGCGTTTTT	CDS
Nedd4L KD #3	TRCN0000000906	CCGGGCGGATGAGAATAGAGA ACTTCTCGAGAAGTTCTCTATT CTCATCCGCTTTTT	CDS
Nedd4L KD #4	TRCN0000000907	CCGGGCGAGTACCTATGAATGG ATTCTCGAGAATCCATTCATAGG TACTCGCTTTTT	CDS
ITCH KD #1	TRCN0000002087	CCGGCCAGAAGTCAAGGTCAAT TAACTCGAGTTAATTGACCTTGA CTTCTGGTTTTT	CDS
ITCH KD #2	TRCN0000002088	CCGGGCCTATGTTCGGGACTTCA AACTCGAGTTTGAAGTCCCGAAC ATAGGCTTTTT	CDS
ITCH KD #3	TRCN0000002090	CCGGCCCAAGAATCAGAGGTTAT ATCTCGAGATATAACCTCTGATT CTTGGGTTTTT	3UTR

Stable Cell Line	shRNA TRC #	Sequence	Target Region
ITCH KD #4	TRCN0000010680	CCGGCGAAGACGTTTGTGGGTGATTCTCGAGAATCACCCACAAACGTCTTCGTTTTT	CDS
Smurf1 KD #1	TRCN0000003471	CCGGGCCCAGAGATACGAAAGAGATCTCGAGATCTCTTTCGTATCTCTGGGCTTTTT	CDS
Smurf1 KD #2	TRCN0000003473	CCGGCTGGAGGTTTATGAGAGGAATCTCGAGATTCCTCTCATAAACCTCCAGTTTTT	CDS
Smurf1 KD #3	TRCN0000003474	CCGGCCGAAGGCTACGAACAAAGAACTCGAGTTCTTTGTTCGTAGCCTTCGGTTTTT	CDS
Smurf1 KD #4	TRCN0000010791	CCGGCGATGGTTTGTTTGGTCCTTTCTCGAGAAAGGACCAAACAAACCATCGTTTTT	3UTR
Smurf2 KD #1	TRCN0000003476	CCGGGTGTGGATACTTGAGAATGATCTCGAGATCATTCTCAAGTATCCACACTTTTT	CDS
Smurf2 KD #2	TRCN0000003477	CCGGCGCCTCAAAGACACTGGTTATCTCGAGATAACCAGTGTCTTTGAGGCGTTTTT	CDS
Smurf2 KD #3	TRCN0000003478	CCGGCCACCCTATGAAAGCTATGAACTCGAGTTCATAGCTTTCATAGGGTGGTTTTT	CDS
Smurf2 KD #4	TRCN0000010792	CCGGGCTGGATTTCTCGGTTGTGTTCTCGAGAACACAACCGAGAAATCCAGCTTTTT	CDS
NedL1 KD #1	TRCN0000001523	CCGGGACCTCACTTTCACTGTTAATCTCGAGATTAACAGTGAAAGTGAGGTCTTTTT	CDS
NedL1 KD #2	TRCN0000001524	CCGGCACCCAGATGATGAGGAGATTCTCGAGAATCTCCTCATCATCTGGGTGTTTTT	CDS
NedL1 KD #3	TRCN0000010637	CCGGGCCTAGACATACGGTGCAAATCTCGAGATTTGCACCGTATGTCTAGGCTTTTT	3UTR

Stable Cell Line	shRNA TRC #	Sequence	Target Region
NedL1 KD #4	TRCN0000010639	CCGGCCGGGACTTGGTGAATTTC ATCTCGAGATGAAATTCACCAAG TCCCGGTTTTT	CDS
NedL2 KD #1	TRCN0000004789	CCGGGCCCAAACATTTCTTTGAA TCTCGAGATCTCAAAGAAATGTT TGGGCTTTTT	3UTR
NedL2 KD #2	TRCN0000004791	CCGGGCACAATACTTGGAGTCAA TTCTCGAGAATTGACTCCAAGTA TTGTGCTTTTT	CDS
NedL2 KD #3	TRCN0000004792	CCGGGCTTACAATGACAAGATTG TTCTCGAGAACAATCTTGTCATT GTAAGCTTTTT	CDS
NedL2 KD #4	TRCN0000004793	CCGGCCCTTATCTTAAGATGTCA ATCTCGAGATTGACATCTTAAGA TAAGGGTTTTT	CDS
WWP1 KD #1	TRCN0000003395	CCGGATTGCTTATGAACGCGGCT TTCTCGAGAAAGCCGCGTTCATA AGCAATTTTTT	CDS
WWP1 KD #2	TRCN0000003397	CCGGTCTGTAACTAAAGGTGGTC CACTCGAGTGGACCACCTTTAGT TACAGATTTTT	CDS
WWP1 KD #3	TRCN0000003398	CCGGCCTCTCAAATTCATAACAG TTCTCGAGAACTGTTATGAATTT GAGAGGTTTTT	3UTR
WWP1 KD #4	TRCN0000010782	CCGGGCTTATTTGAGTATGCGGG CACTCGAGTGCCCGCATACTCAA ATAAGCTTTTT	CDS
WWP2 KD #1	TRCN0000001512	CCGGGTTTGTTAGGTTTGCCAGG TTCTCGAGAACCTGGCAAACCTA ACAAACTTTTT	3UTR
WWP2 KD #2	TRCN0000001513	CCGGCGGCACAGAGTCATTTAGA TTCTCGAGAATCTAAATGACTCT GTGCCGTTTTT	CDS
WWP2 KD #3	TRCN0000001514	CCGGCCTCACCTACTTTCGCTTTA TCTCGAGATAAAGCGAAAGTAG GTGAGGTTTTT	CDS

Stable Cell Line	shRNA TRC #	Sequence	Target Region
WWP2 KD #4	TRCN0000001515	CCGGCCCAAGGTGCATAATCGTC AACTCGAGTTGACGATTATGCAC CTTGGGTTTTT	CDS
TRC1 Empty Vector	SHC001	No shRNA insert	-